BRNO UNIVERSITY OF TECHNOLOGY

Faculty of Electrical Engineering
and Communication

MASTER'S THESIS

Brno, 2021

Bc. Jiří Křivák

BRNO UNIVERSITY OF TECHNOLOGY

VYSOKÉ UČENÍ TECHNICKÉ V BRNĚ

FACULTY OF ELECTRICAL ENGINEERING AND COMMUNICATION

FAKULTA ELEKTROTECHNIKY
A KOMUNIKAČNÍCH TECHNOLOGIÍ

DEPARTMENT OF RADIO ELECTRONICS

ÚSTAV RADIOELEKTRONIKY

ANALYSIS OF FEEDING TECHNIQUES OF A PATCH ANTENNA ARRAY FOR 5G NR

ANALYSIS OF FEEDING TECHNIQUES OF A PATCH ANTENNA ARRAY FOR 5G NR

MASTER'S THESIS
DIPLOMOVÁ PRÁCE

AUTHOR
AUTOR PRÁCE

Bc. Jiří Křivák

SUPERVISOR
VEDOUCÍ PRÁCE

prof. Dr. Ing. Christoph Mecklenbräuker
VIENNA UNIVERSITY OF TECHNOLOGY

doc. Ing. Jaroslav Láčík, Ph.D.
BRNO UNIVERITY OF TECHNOLOGY

BRNO 2021

BRNO UNIVERSITY OF TECHNOLOGY
FACULTY OF ELECTRICAL ENGINEERING AND COMMUNICATION

Master's Thesis

Master's study program **Telecommunications**

Department of Radio Electronics

Student: Bc. Jiří Křivák ***ID:*** 186122

Year of study: 2 ***Academic year:*** 2020/21

TITLE OF THESIS:

Analysis of feeding techniques of a patch antenna array for 5G NR

INSTRUCTION:

The goal of the diploma thesis is to analyze different feeding structures of 2x2 microstrip patch antenna arrays with center frequency of 25.5 GHz. The thesis shall include:

1. Comparison of feeding techniques of 2x2 planar array
2. Three different feeding techniques
3. Center frequency at 25.5 GHz
4. Two different PCB substrates

RECOMMENDED LITERATURE:

[1] BALANIS, Constantine A. Antenna Theory: Analysis and Design. 4th ed. Wiley, 2016. ISBN 978-1-118-64-06-1.

[2] BALANIS, Constantine A. Fundamental Parameters and Definitions for Antennas. Wiley Telecom, 2008. ISBN 9781118209752.

Date of project specification: 8.2.2021 ***Deadline for submission:*** 5.8.2021

Supervisor: doc. Ing. Jaroslav Láčík, Ph.D.
Consultant: Dr. Ing. Christoph Mecklenbräuker

doc. Ing. Tomáš Frýza, Ph.D.
Chair of study program board

ABSTRACT

The goal of this thesis is to analyze different feeding structures of two by two microstrip patch antenna arrays. The evaluation centre frequency is $25.5GHz$. This frequency falls into the range assigned to the fifth generation mobile communication standard.
This thesis focuses on the design and simulation of microstrip patch antenna arrays fed by proximity feeding structure, aperture coupled feeding structure and the inset microstrip line feeding structure. These antennas and their feeding structures are simulated with two different dielectric PCB substrates.

KEYWORDS

2x2 patch antenna array, feeding structures, inset-fed, proximity-fed, aperture-fed

KŘIVÁK, Jiří. *Analysis of feeding techniques of a patch antenna array for 5G NR*. Brno: Brno University of Technology, Faculty of Electrical Engineering and Communication, Department of Telecommunications, 2021, 96 p. Master's Thesis. Advised by prof. Dr. Ing. Christoph Mecklenbräuker

Author's Declaration

Author:	Bc. Jiří Křivák
Author's ID:	186122
Paper type:	Master's Thesis
Academic year:	2020/21
Topic:	Analysis of feeding techniques of a patch antenna array for 5G NR

I declare that I have written this paper independently, under the guidance of the advisor and using exclusively the technical references and other sources of information cited in the paper and listed in the comprehensive bibliography at the end of the paper.

As the author, I furthermore declare that, with respect to the creation of this paper, I have not infringed any copyright or violated anyone's personal and/or ownership rights. In this context, I am fully aware of the consequences of breaking Regulation § 11 of the Copyright Act No. 121/2000 Coll. of the Czech Republic, as amended, and of any breach of rights related to intellectual property or introduced within amendments to relevant Acts such as the Intellectual Property Act or the Criminal Code, Act No. 40/2009 Coll. of the Czech Republic, Section 2, Head VI, Part 4.

Brno ....

author's signature*

*The author signs only in the printed version.

ACKNOWLEDGEMENT

I would like to thank the co-advisor of my thesis from Technical University of Wien, Dipl.-Ing. Dr.techn Robert Langwieser, for his valuable comments.

Contents

List of Figures

List of Tables

Introduction

With the rise of the fifth-generation mobile communication network comes the necessity to design systems operating in the millimeter wavelength. One of such systems is the antenna. The 5G NR, where the 5G stands for the 5th generation of mobile communication, and the NR stands for new radio. The 5G NR is composed of two frequency ranges. The first range consists of sub-6 GHz frequencies, and the second frequency range has frequencies allocated to it in the above 20 GHz frequency range.

5G NR Band	Band Alias	Uplink / Downlink Band	Bandwidth	Type
n257	28 GHz	26.5 - 29.5 GHz	3 GHz	TDD
n258	26 GHz	24.250 - 27.5 GHz	3.250 GHz	TDD
n259	-	39.5 - 43.5 GHz	4 GHz	TDD
n260	39 GHz	37 - 40 GHz	3 GHz	TDD
n261	28 GHz	27.5 - 28.35 GHz	850 MHz	TDD

Tab. 1: 5G NR extended frequency bands

For this thesis, the evaluation frequency was selected at 25.5 GHz. As can be seen in table 1, this evaluation frequency belongs to the n258 frequency band, which ranges from 24.250 to 27.5 GHz.

For applications such as measurements in this frequency, a good antenna array is required, but the question is what feeding technique such array should implement, and this is the focus of this thesis. The analysis of feeding techniques of a patch antenna array for 5G NR.

There are numerous ways how to feed patch antenna and patch antenna arrays, so this thesis focuses only on a few of them. The selected feeding techniques in this thesis are the following:

- Inset feeding technique
- Proximity feeding technique
- Aperture feeding technique

In this thesis, the comparison of the patch antenna arrays is done for the condition that the separation of the ground plane from the patch antenna is the same for all types of feeding or close as the same when the standard dimensions of substrates are taken into account.

1 Theory

This chapter contains the theoretical background pertaining to this master thesis.

First, there is some information about the design of microstrip transmission lines, then there is information about the design of the rectangular patch antenna.

This chapter discusses different feeding techniques, antenna parameters, and the introduction of antenna arrays.

1.1 Microstrip line

One of the commonly used methods of signal delivery on printed circuit boards is the use of microstrip lines.

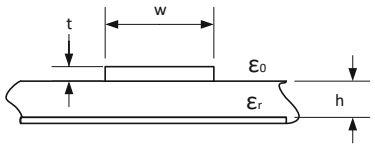

Fig. 1.1: Microstrip line

The important parameter of the transmission line is the *characteristic impedance* (Z_0). Figure 1.1 shows the cross-section of the microstrip line and the dimensions and material properties used in the calculation of the microstrip line. These dimensions are the *width of the microstrip line* (w),*height of the substrate* (h). The material properties used in calculation of microstrip lines are *relative permittivity* (ϵ_r) and *permittivity of vacuum* (ϵ_0).

The dimensions can be calculated by the set of following equations: For high impedance microstrip line $Z_0 > (44 - 2\epsilon_r)\Omega$ the following formula can be used [3]

$$\frac{w}{h} = (\frac{e^{H'}}{8} - \frac{1}{4\exp H'})^{-1} \tag{1.1}$$

where [3]

$$H' = \frac{Z_0\sqrt{2(\epsilon_r+1)}}{119.9} + \frac{1}{2}(\frac{\epsilon_r-1}{\epsilon_r+1})(\ln\frac{\pi}{2} + \frac{1}{\epsilon_r}\ln\frac{4}{\pi}) \tag{1.2}$$

For low impedance microstrip line $Z_0 < (44 - 2\epsilon_r)\Omega$ the following formula can be used [3]

$$\frac{w}{h} = \frac{2}{\pi}[(B-1) - \ln(2B-1)] + \frac{(\epsilon_r-1)}{\pi\epsilon_r}[\ln(2B-1) + 0.293 - \frac{0.517}{\epsilon_r}] \tag{1.3}$$

where [3]

$$B = \frac{59.95\pi^2}{Z_0\sqrt{\epsilon_r}} \tag{1.4}$$

Because there are two different dielectric environments the waves propagate in *hybrid electromagnetic* (HEM) mode. On lower frequencies the wave can be approximated as *transverse electromagnetic* (TEM) wave. Because the approximation is used it is necessary to calculate *effective permittivity* (ϵ_{eff}) which is actually the effective relative permittivity.

The ϵ_{eff} is calculated by the following equations[3]

$$\epsilon_{\text{eff}} = \frac{\epsilon_r + 1}{2} + \frac{\epsilon_r - 1}{2}\left[\frac{1}{\sqrt{1 + 12(\frac{h}{w})}} + 0.04\left(1 - \frac{w}{h}\right)^2\right] \tag{1.5}$$

for $w/h < 1$ and for $w/h > 1$ the following is used[3]

$$\epsilon_{\text{eff}} = \frac{\epsilon_r + 1}{2} + \left[\frac{\epsilon_r - 1}{2\sqrt{1 + 12(\frac{h}{w})}}\right] \tag{1.6}$$

1.2 Patch antenna design

1.2.1 Types of patch antennas

There are multiple types of patch antennas. Based on their geometry, the most common types of patch antennas are:

- Square
- Rectangle
- Circle
- Ellipse

There are other types of patch antennas based on other elemental geometries, such as triangles, but the majority is based on the most common types, with or without some modifications. Such modifications pertain to cutting out slots or other geometrical elements, such as cutting out a rectangle from a rectangular antenna gives us an H-type patch or U-type patch antennas[1].

1.2.2 Rectangular patch antenna

Microstrip patch antenna consists of a thin metallic patch above metallic ground separated by a thin layer of a dielectric substrate. This dielectric substrate has a h, which is a small fraction of the resonant wavelength at which the antenna resonates $h \ll \lambda_0$.

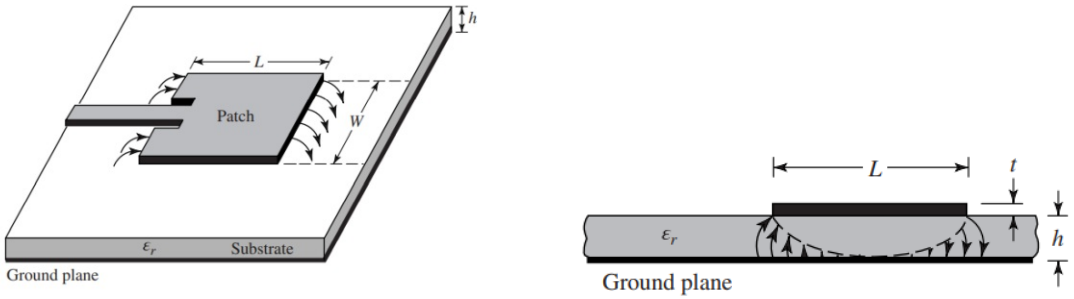

(a) 3D view (b) Side view

Fig. 1.2: Patch antenna [1]

Because figure 1.2 is taken from [1] W is the *width of the patch* (W_p), and L is the *length of the patch* (L_p) in this thesis.

Patch antenna can be considered as two radiating apertures of length W_p and height h, separated by low impedance microstrip line of length L_p. The distribution of the electric field responsible for the radiation can be seen in figure 1.2, and it is represented by the vector arrows. From this, it is apparent that the radiation happens at the edges of the patch antenna.

For calculating W_p the following equation is used[1]:

$$W_{\mathrm{p}} = \frac{c_0}{2f_{\mathrm{r}}}\sqrt{\frac{2}{\epsilon_{\mathrm{r}}+1}} \tag{1.7}$$

where the c_0 is *speed of the light* (C_0), *resonant frequency* (f_{r}), and the ϵ_{r}.

As the next step, the ϵ_{eff} is calculated with the following equation[1]

$$\epsilon_{\mathrm{eff}} = \frac{\epsilon_r+1}{2} + \frac{\epsilon_r-1}{2}[1+12\frac{h}{W_p}]^{-1/2} \tag{1.8}$$

then the *effective length of the patch* (L_{eff}) can be calculated using [1]

$$L_{\mathrm{eff}} = \frac{c_0}{2f_r\sqrt{\epsilon_{\mathrm{eff}}}} \tag{1.9}$$

To get the L_p the *length extension* (ΔL) needs to be calculated first[1]

$$\frac{\Delta L}{h} = 0.412 \times \frac{(\epsilon_{\mathrm{eff}}+0.3)(\frac{W_p}{h}+0.264)}{(\epsilon_{\mathrm{eff}}-0.258)(\frac{W_p}{h}+0.8)} \tag{1.10}$$

and then the L_p can be calculated using the following equation[1]

$$L_p = L_{\mathrm{eff}} - 2\Delta L \tag{1.11}$$

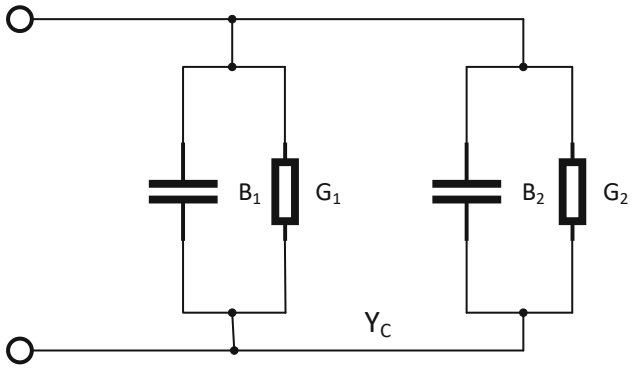

Fig. 1.3: Patch antenna transmission model equivalent circuit

Figure 1.3 shows the transmission model equivalent circuit. It can be seen that the radiating slots are represented by pair of parallel equivalent admittances Y. Each admittance has conductance G and susceptance B. These admittances are used in

calculation of the *edge resistance* (R_{in}) of the patch antenna, which is given by the following equation[1]

$$R_{\text{in}} = \frac{1}{2G_1} \tag{1.12}$$

where conductance G_1 is given by the following[1]

$$G_1 = \frac{W_p}{120\lambda_0}\left[1 - \frac{1}{24}(k_0 h)^2\right] \tag{1.13}$$

Additionally, the R_{in} can be approximated by the following equation[1]

$$R_{\text{in}} = 90\frac{(\epsilon_r)^2}{\epsilon_r - 1}\frac{L_p}{W_p} \tag{1.14}$$

this expression is an approximation that is valid for $h \ll \lambda_0$[1].

1.3 Feeding methods of patch antennas

Various feeding techniques can feed the microstrip patch antenna. The following feeding techniques listed are just some of the basic patch antenna feeding techniques.

1.3.1 Coaxial probe-fed patch antenna

The coaxial probe fed patch antenna is fed by a coaxial probe from the bottom side of the patch.

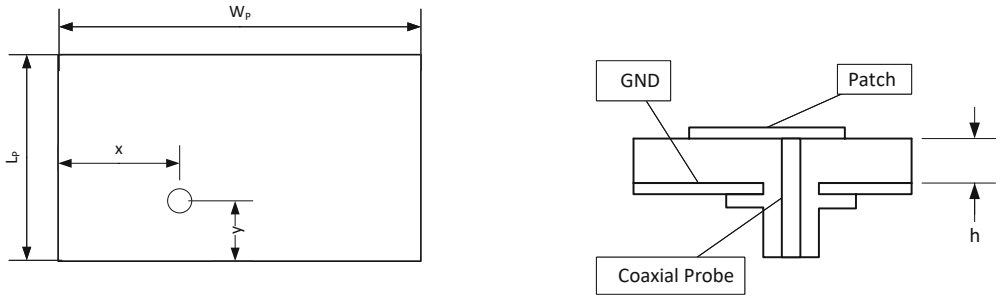

(a) Top view (b) Side view

Fig. 1.4: Coaxial probe-fed patch

The location of probe is related to the edge resistance R_{in}, the resistance decreases with the distance from the edge of the antenna. The location of the feeding

point is defined by x_0 and y_0 as can be seen in figure 1.4(a) and is calculated by the following equations [4]

$$x_0 = \frac{L_p}{\sqrt{\epsilon_{\text{eff}}}}; y_0 = \frac{W_p}{2} \tag{1.15}$$

The dimensions W_p and L_p can be calculated by the equations 1.7 and 1.11 respectively [4].

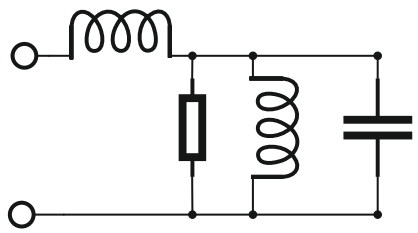

Fig. 1.5: Probe-fed equivalent circuit

Figure 1.5 shows the equivalent circuit of the probe-fed patch antenna. From the circuit it can be seen that the coaxial probe feeding is inductive.

1.3.2 QWIT-fed patch antenna

The QWIT-fed patch antenna is a patch antenna fed through a *Quarter Wave Impedance Transformer* (QWIT).

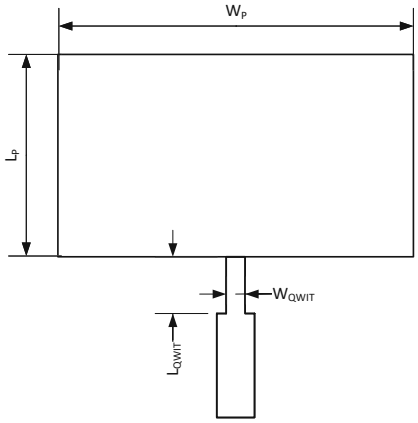

Fig. 1.6: QWIT-fed patch

Figure 1.6 shows the QWIT-fed patch antenna, where the W_{QWIT} is the width of the quarter wave impedance transofrmer and the L_{QWIT} is its length.

The principle of the QWIT matching is that the edge impedance of the patch antenna is matched to the microstrip line using a quarter-wave impedance transformer.

For impedance matching, the edge impedance of the patch antenna is calculated using the equation 1.12. Then the impedance of the QWIT is calculated to match the impedance of the microstrip line. That is done by the following equation[5]:

$$Z_{0,\lambda/4} = \sqrt{Z_{\mathrm{in}} Z_{\mathrm{A}}} \tag{1.16}$$

where the Z_{in} is the impedance at the input, in this case the microstrip line, and the Z_{A} is the edge impedance of the antenna, this formula is valid under the condition that the length of the matching line is that quarter of the wavelength, so that $L_{\mathrm{QWIT}} = \lambda_{\mathrm{g}}/4$. This is calculated as the guided wavelength of the microstrip patch and is given by the following equation[6]

$$\lambda_g = \frac{\lambda_0}{\sqrt{\epsilon_{\mathrm{eff}}}} \tag{1.17}$$

where λ_0 is the wavelength in the vacuum and ϵ_{eff} is the effective relative permitivity as given by equation 1.5 or the 1.6.

1.3.3 Inset-fed patch antenna

One of the most commonly used methods of feeding microstrip patch antennas is the inset feeding.

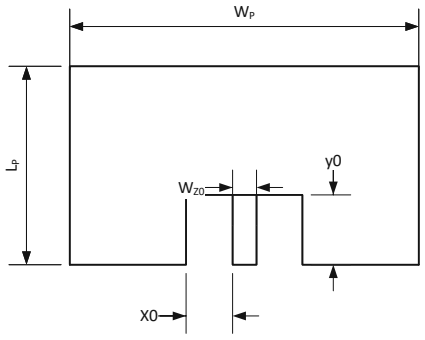

Fig. 1.7: Inset-fed patch

In the figure 1.7, the inset-fed microstrip patch antenna can be seen. The microstrip patch antenna is fed by microstrip line of width W_{Z0}, directly connected to the patch antenna. The matching principle is that the impedance of the microstrip patch antenna increases with the distance from the centre of the antenna. The antenna has a rectangular cutout that allows the feeding microstrip line to connect in position that has same impedance value as the characteristic impedance of the feeding microstrip line.

As was mentioned before,for the microstrip patch antennas, the impedance increases with the distance from the center of the patch. This can be expressed by the following equation [1]

$$R_{\text{in}}(y = y_0) = R_{\text{in}}(y = 0)cos^2(\frac{\pi}{L_p}y_0) \tag{1.18}$$

From that, the equation for the distance can be expressed as the following

$$y_0 = \frac{L_p}{\pi}\arccos(\sqrt{\frac{R_{\text{in}}(y = y0)}{R_{\text{in}}(y = 0)}}) \tag{1.19}$$

where $R_{\text{in}}(y = 0)$ is the edge resistance in resonance of the patch antenna given by the 1.12 and the $R_{\text{in}}(y = y0)$ is the resistance of the feeding line[1].

1.11 respectively [4].

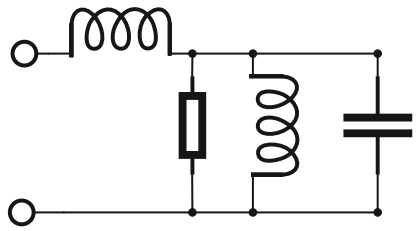

Fig. 1.8: Inset-fed equivalent circuit

Figure 1.8 shows the equivalent circuit of the inset-fed patch antenna. From the circuit it can be seen that the inset feeding is inductive. Also the equivalent circuit is same as in the case of the coaxial probe feeding, this is reflected in the fact that the matching is done by same principle. By finding the location of equivalent resistance, which increase from the centre of the patch antenna.

1.3.4 Proximity-fed patch antenna

Another feeding method is the proximity feeding.

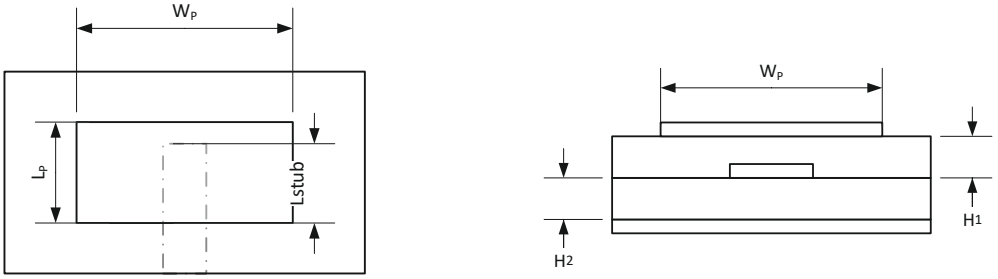

(a) Top view (b) Side view

Fig. 1.9: Proximity-fed patch

As can be seen in figure 1.9, the proximity-fed patch antenna is a multi-layer patch antenna. The patch antenna is etched at the top layer of the substrate. The feeding microstrip line is embedded between two layers of dielectric PCB substrates, with substrate heights H_1 and H_2. At the bottom of the structure is the ground plane.

At the proximity-fed patch antenna, feeding is done by running an open-ended microstrip line under the radiating patch. The matching is done by varying the *length of the stub* (L_{stub}) of the microstrip line. 1.11 respectively [4].

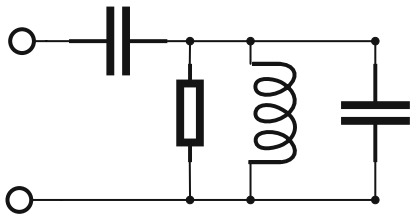

Fig. 1.10: Proximity-fed equivalent circuit

Figure 1.10 shows that the proximity feeding is capacitive. This means that distances H_1 and affect H_2 the capacitance. With the increase of the distance H1 the capacitance decreases.

[7]

1.3.5 Aperture-fed patch antenna

The last mentioned feeding method is the aperture feeding.

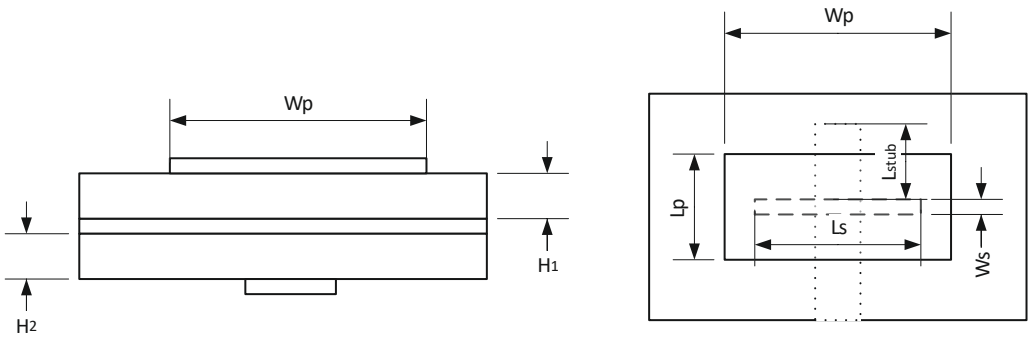

Fig. 1.11: Aperture-fed patch

The aperture-fed patch antenna is a multi-layer patch antenna. The antenna consists of the patch antenna, slot in the ground layer, and microstrip line. There can be many variations of this coupling.

For this type of feeding, the *length of the slot* (L_S) determines the coupling as well back lobe radiation level. The *width of the slot* (W_S) also affects coupling but to a much lesser extent than slot length and is usually set as one-tenth of the length of the slot. These dimensions also affects the resonating frequency to a small degree.

The position of the slot is at the center of the patch antenna, and the feed line is perpendicular to the center of the slot.

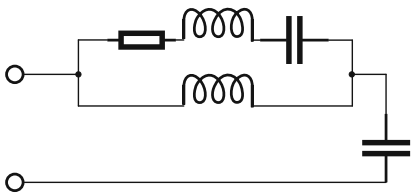

Fig. 1.12: Proximity-fed equivalent circuit

Figure 1.12 shows that the aperture feeding is resonant feeding.[8]

1.4 Antenna parameters

1.4.1 Scattering parameters and Voltage Standing Wave Ratio

S parameters, which is short for scattering parameters, they describe the high frequency circuit in terms of waves. They are defined for an N-Port device and are represented by the s parameter matrix. For antenna measurements, the most important parameter is $S_{1,1}$ which represents reflected waves of a circuit terminated by matched load at circuit input port.

The $S_{1,1}$ is also called the *reflection coefficient* (Γ) and it can be described by the following formula [1]

$$\Gamma = \frac{Z_{\text{in}} - Z_0}{Z_{\text{in}} + Z_0} \tag{1.20}$$

where the Z_{in} is the impedance at the input of the antenna and the Z_0 is the characteristic impedance of the transmission line.

The *voltage standing wave ration* (VSWR) is the ratio of the peak amplitude of a standing wave to the minimum amplitude of a standing wave, this can also be described using Γ using the following formula [1].

$$VSWR = \frac{1+ \mid \Gamma \mid}{1- \mid \Gamma \mid} \tag{1.21}$$

[9][1].

1.4.2 Input impedance

Input impedance is the impedance presented by the antenna at its terminal. It is defined by the following formula[1]

$$Z_A = R_A + jX_a \tag{1.22}$$

whereZ_A is the antenna impedance, R_A is antenna resistance and X_A is the antenna reactance.

$$R_A = R_R + R_L \tag{1.23}$$

where the R_R is the radiation resistance of the antenna and the R_L is the loss resistance of the antenna [1].

1.4.3 Antenna equivalent area

There are several equivalent areas associated with antennas. They describe power capturing characteristics. One is the effective area, which is defined as *"the ratio of the available power at the terminals of a receiving antenna to the power flux*

density of a plane wave incident on the antenna from that direction, the wave being polarization-matched to the antenna. If the direction is not specified, the direction of maximum radiation intensity is implied"[1].

The *effective equivalent area* (A_e) can be written as the following formula [1]

$$A_e = \frac{P_T}{W_i} \tag{1.24}$$

where the A_e is the effective area, the P_T is the power delivered to the load, the W_i is the power density of the incident wave. This can also be written as [1]

$$A_e = \frac{\mid V_T \mid^2}{8W_i}\left[\frac{R_T}{(R_R + R_L + R_T)^2 + (X_A + X_T)^2}\right] \tag{1.25}$$

where V_T is the voltage induced by the incident wave, R_T is resistance of the load and X_T is the inductance of the load.

The maximum effective area can be defined by the following formula [1]

$$A_{\mathrm{e,max}} = \frac{\mid V_T \mid^2}{8W_i}\left[\frac{1}{R_r + R_L}\right] \tag{1.26}$$

the maximum effective area is related to the directivity of the antenna, this can be described by the following equation[1]

$$A_e = \eta_0(\frac{\lambda^2}{4\pi})D_{\mathrm{max}} \tag{1.27}$$

where the η_0 is the total antenna efficiency, D_{max} is maximum directivity and λ is the wavelength.

From the effective area of the antenna the antenna *aperture efficiency* (ϵ_{AP}) can be estimated by the following equation [1]

$$\epsilon_{\mathrm{AP}} = \frac{A_{\mathrm{e,max}}}{A_p} \tag{1.28}$$

where A_P is the physical area of the antenna [1].

1.4.4 Radiation pattern

An antenna radiation pattern or antenna pattern is defined as "a mathematical function or a graphical representation of the radiation properties of the antenna as a function of space coordinates"[10].

It can be represented by function $F(\theta, \phi)$, which is represented in the coordinate system. Commonly the radiation pattern is described by two dimensional graphical representation, using cuts in the 3d radiation pattern. From this pattern the parameters as beam-width, side lobe level and front to back ratio are calculated [10].

1.4.5 Beam-width

Beam-width is the angle between two points with identical values on pattern taken in same plane.

Half power beam-width is defined by IEEE as *"In a plane containing the direction of the maximum of a beam, the angle between the two directions in which the radiation intensity is one-half value of the beam"*[11].

Front to Back ratio

Front-to-Back Ratio is defined as *"the ratio of the maximum directivity of an antenna to its directivity in a specified rearward direction"* [11].

Side lobe level

Side Lobe level is defined as *"the ratio of the radiation intensity of a side lobe in the direction of its maximum value to that of the intended lobe, usually expressed in decibels"* [11].

1.4.6 Efficiency

In antenna system there are several efficiencies. The *overall efficiency* (η_0) can be defined as the following formula[1]

$$\eta_0 = \eta_r \eta_c \eta_d \tag{1.29}$$

Where η_0 is total efficiency, η_r is the reflection efficiency, η_c is conduction efficiency and η_d is dielectric efficiency.

Where the *reflection efficiency* (η_r) is given by the following equation[1]

$$\eta_r = (1 - \mid \Gamma \mid)^2 \tag{1.30}$$

where Γ is the reflection coefficient.[1] The conduction-dielectric efficiency is the combined efficiencies of η_c and η_d, it is sometimes also called antenna radiation efficiency. It is defined as the ratio of the power delivered to the radiation resistance R_R to the power delivered to antenna resistance R_A this is described in the following formula [1]:

$$\eta_{\text{cd}} = \frac{R_R}{R_A} \tag{1.31}$$

[1].

1.4.7 Directivity

Directivity is defined as *"the ratio of the radiation intensity in a given direction from the antenna to the radiation intensity averaged over all directions."*[11]

Directivity $D(\theta, \phi)$ can be expressed as the ratio of the *radiation intensity* $(U(\theta, \phi))$ in a certain direction to the average radiation intensity over all directions[1]

$$D(\theta, \phi) = \frac{U(\theta, \phi)}{U_{\text{Avg}}} \tag{1.32}$$

and for the maximum value[1]

$$D_{\max} = \frac{U_{\max}}{U_{\text{Avg}}} = \frac{U(\theta_{\max}, \phi_{\max})}{U_{\text{Avg}}} \tag{1.33}$$

Where $U_{\max}$ is the maximum radiation intensity of the given antenna and U_{Avg} is radiation intensity that isotropic source would radiate. Which can be defined as[1]:

$$U_{\text{Avg}} = \frac{P_{\text{Rad}}}{4\pi} \tag{1.34}$$

where the P_{Rad} is the total radiated power of the antenna [1].

1.4.8 Gain

The gain of an antenna is defined as *"The ratio of the radiation intensity in a given direction to the radiation intensity that would be produced if the power accepted by the antenna were isotropically radiated"*[11].

The *gain* $(G(\theta, \phi))$ is defined as [1]

$$G(\theta, \phi) = \frac{4\pi U(\theta, \phi)}{P_{\text{In}}} \tag{1.35}$$

and the *peak gain* $(G_{\max})$ as [1]

$$G_{\max} = \frac{4\pi U(\theta_{\max}, \phi_{\max})}{P_{\text{In}}} \tag{1.36}$$

where the P_{In} is the power at the input of the antenna. This power is related to the *radiated power* (P_{Rad}) by the following formula[1]

$$P_{\text{Rad}} = \eta_{\text{cd}} P_{\text{In}} \tag{1.37}$$

. So it can be seen that the antenna gain is closely related to the directivity, but it also takes into account the radiation efficiency. Thus it can be defined by the following formula [1]

$$G(\theta, \phi) = \eta_{\text{cd}} D(\theta, \phi) \tag{1.38}$$

We can also specify the maximum value [1]

$$G_{\max} = \eta_{\text{cd}} D_{\max} \tag{1.39}$$

While useful, the gain doesn't take into account the losses caused by the impedance mismatch. For that reason, the *realized gain* ($G_{\text{re}}(\theta, \phi)$) is used, which is a gain definition that takes the transmission losses in to account and it can be formulated as the following [1]

$$G_{\text{re}}(\theta, \phi) = \eta_{\text{r}} G(\theta, \phi) = \eta_r \eta_{\text{cd}} D(\theta, \phi) = \eta_0 D(\theta, \phi) \tag{1.40}$$

and similarly the *peak realized gain* ($G_{\text{re,max}}$) as[1]

$$G_{\text{re,max}} = \eta_{\text{r}} G(\theta, \phi) = \eta_0 D(\theta, \phi) \tag{1.41}$$

[1].

1.4.9 Polarization

The polarization of the antenna is given by the polarization of the wave radiated by said antenna.

Polarization of a radiated wave is defined as *"that property of an electromagnetic wave describing the time-varying direction and relative magnitude of the electric-field vector; specifically, the figure traced as a function of time by the extremity of the vector at a fixed location in space, and the sense in which it is traced, as observed along the direction of propagation"*[11].

We can categorize polarization of the wave as linear, circular or elliptical.

As mention in the definition electromagnetic waves are represented by their electric field vectors, for linear polarization this field vector has to have only one component.

For circularly polarized wave its electric field vector has to trace circle as a function of time for that the field vector has to have two orthogonal components of same magnitude and a phase difference of odd multiples of 90°.

Elliptically polarized wave is, if it is neither linearly nor circularly polarized wave, and the electric field vector has two orthogonal components, which can vary in magnitude. [1].

Cross polarization

The cross polarization is defined as *"the polarization orthogonal to a reference polarization"*[11].

For such case, one of the used references is the Ludwig's third definition of polarization, as it is defined based on typical antenna measurement of polarization as can be seen in the figure 1.13

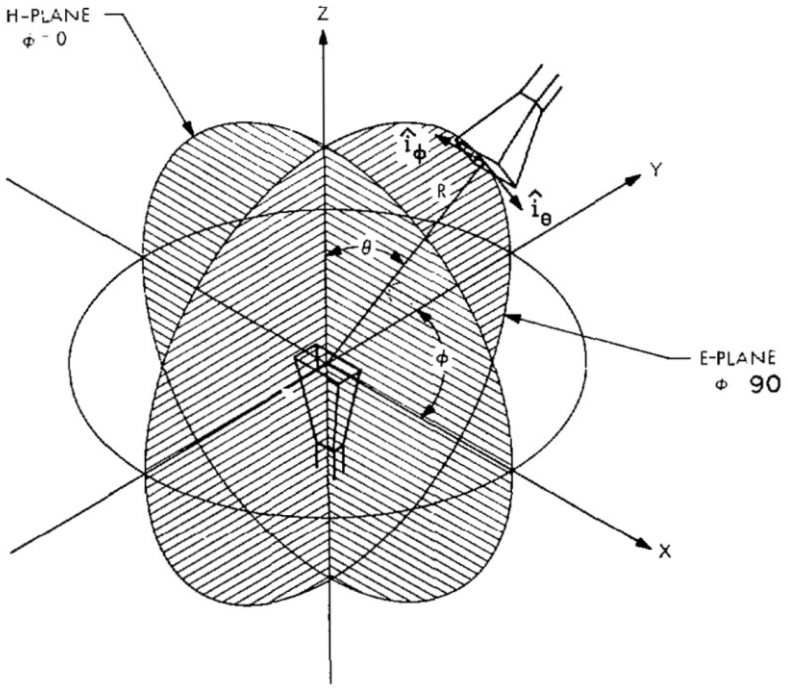

Fig. 1.13: Antenna polarisation measurement[2]

where the antenna is placed at the origin x,y,z space and the measurement antenna traverse great circle around the measured antenna. The measured electric field consists of two components, that of co polarized and cross polarized components. This can be written as [12]

$$E_{\text{co}} = \bar{E} \cdot \bar{u}_{\text{co}}^{(3)} \tag{1.42}$$

and [12]

$$E_{\text{cross}} = \bar{E} \cdot \bar{u}_{\text{cross}}^{(3)} \tag{1.43}$$

where $\bar{E}$ is electric field vector and u_{co} and u_{cross} are unit vectors dependent on selected reference and its orientation.

Ludwig's third definition of reference polarization is defined by the following equations [12]

$$\bar{u}_{\text{co}}^{(3)} = \sin\phi\,\hat{\theta} + \cos\phi\,\hat{\phi} \tag{1.44}$$

for polarization pattern and [12]

$$\bar{u}_{\text{cross}}^{(3)} = \cos\phi\,\hat{\theta} - \sin\phi\,\hat{\phi} \tag{1.45}$$

for cross polarization pattern.Where the $\hat{\theta}$ and $\hat{\phi}$ are the unit vectors that represent the theoretical and measured fields radiated by an antenna, in a spherical coordinate system.

The reference for the Ludwig-3 definition of polarization is the Huygens source, oriented along the y- and x-axes. The Huygens source is considered an ideal electromagnetic source that radiates with orthogonal electric fields in any direction and with zero cross polarization[12].

1.5 Antenna array

An antenna array is a group of antenna elements working together, and for far-field observers, they appear as a singular antenna element.

1.5.1 Array factor

Each array has its own array factor, and the array factor function is given by the geometry of the array and excitation phase. By varying phases of excitation and distance between the elements, the total resulting field of the array can be controlled. The electrical intensity at the observation point in space is given as the product of the electrical intensity of the antenna element and the array factor and thus can be defined as the following [1]:

$$E_{\mathrm{t}}(\theta, \phi) = E_{\theta,\phi} \cdot AF(\theta, \phi) \tag{1.46}$$

where E_{t} is the total resulting electric field, the $E_{\theta,\phi}$ is the electric field of the single antenna element and $AF(\theta, \phi)$ is the array factor function. For example, for the linear M-element array arranged along the axis x, the array factor can be formulated as [1]

$$AF(\theta, \phi) = \sum_{\mathrm{m}=1}^{M} \exp^{j(m-1)\psi} \tag{1.47}$$

$$\psi = kd \sin(\theta) \cos(\phi) + \beta \tag{1.48}$$

where k is the wavenumber $k = 2\pi/\lambda$, d is the distance of the elements, and β is the phase difference between two neighboring elements.[1]

1.5.2 Array types

When considering microstrip patch antennas, the following array configurations are the most typical.

Linear arrays

A linear antenna array is defined as *"an array antenna having the centers of the radiating elements lying along a straight line.*[11]

For linear M-element array, arranged along the axis x, the array factor can be formulated as [1]

$$AF(\theta, \phi) = \sum_{\mathrm{m}=1}^{M} I_{\mathrm{m1}} \exp^{\mathrm{j(m-1)kd_x \sin\theta \cos\phi + \beta_x}} \tag{1.49}$$

where k is the wave number $k = 2\pi/\lambda$, d_x is the distance of the the elements, the β_x is the phase difference between two neighboring elements and I_{m1} is excitation coefficient of each antenna element.

Planar arrays

A planar array antenna is defined as *"an array antenna having the centers of the radiating elements lying in a plane."*[11] Planar arrays offer higher versatility in design and offer more symmetrical radiation patterns. An additional benefit is when used in scanning arrays, the scanning direction is two-dimensional. For planar arrays, with $M \times N$ antenna elements, the array factor of linear arrays can be extended to [1]

$$AF(\theta,\phi) = \sum_{n=1}^{N} I_{1n}[\sum_{m=1}^{M} I_{m1}\,\mathrm{exp}^{\mathrm{j}(m-1)\mathrm{kd_x}\sin\theta\cos\phi+\beta_x}]\,\mathrm{exp}^{\mathrm{j}(n-1)\mathrm{kd_y}\sin\theta\sin\phi+\beta_y} \tag{1.50}$$

this is an extension of the linear array factor along the axis y, where I_{m1} and I_{1n} are excitation coefficients of each antenna element.

Broadside array

The broadside array has its radiation directed to the norm of the axis of the array.[1]

End-fire array

The end-fire array has its radiation directed along the axis of the array.[1]

Phased array

By controlling the phase difference between the concurring elements, the direction of the radiation can be steered. In linear arrays, the steering is one dimensional, and in a planar array, the steering becomes two dimensional.[1]

1.5.3 Array feeding

Series Feeding

Series array feeding is when individual antenna elements are connected in series. This technique is limited to arrays with fixed beam, or arras that are scanned by frequency.

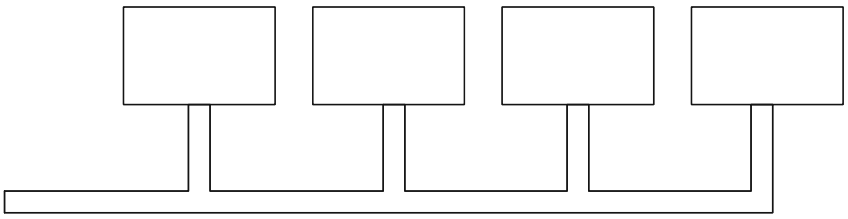

Fig. 1.14: Out-of-line series fed patch antenna array

In figure 1.14, the out of line series fed patch antenna array can be seen. This is a form of linear array fed in series, where the feeding is out of line. This configuration minimizes the mutual dependency of the patches.

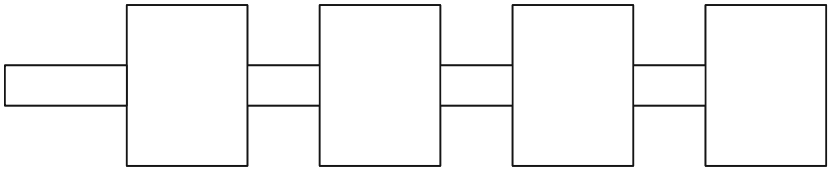

Fig. 1.15: In-line series fed patch antenna array

In figure 1.15, the in line series fed patch antenna array can be seen. In this configuration the antenna elements are very dependent on each other. This means that changes to single element affects all elements.

Parallel

Parallel feeding, sometimes called corporate, is when antennas elements are fed in parallel. Parallel fed arrays exhibit greater versatility over series fed array. They can be made that they have multiple beams and that they can be scanned by variation of phase.

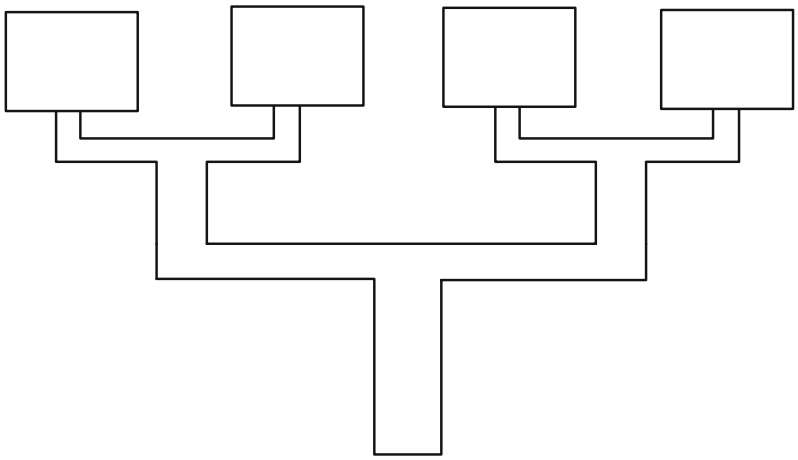

Fig. 1.16: Parallel fed patch antenna array

In figure 1.16, the parallel fed patch antenna array can be seen. In this case it is four element linear array.

Hybrid

Hybrid feeding is when a combination of series and parallel are put together.

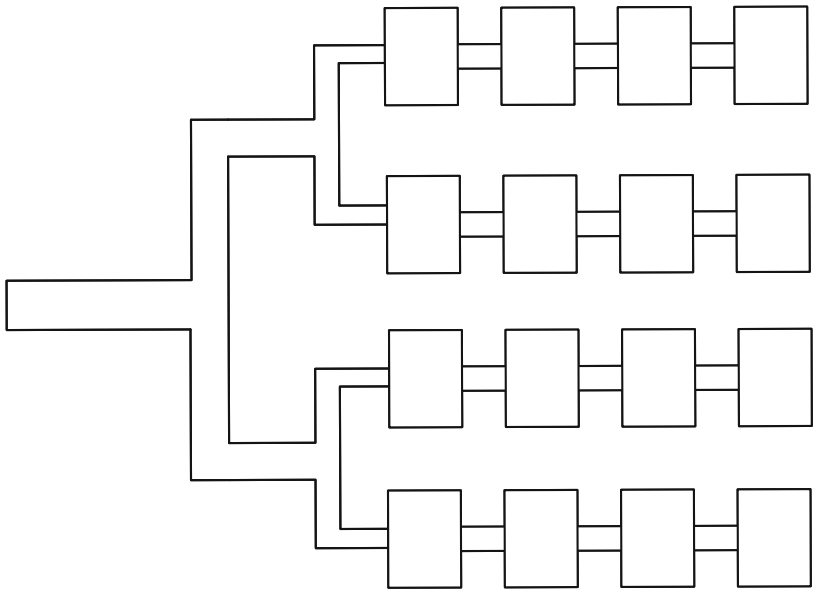

Fig. 1.17: Hybrid fed patch antenna array

In figure 1.17, the hybrid feeding structure can be seen. In this case it shows planar array that is bade of 4 series fed linear arrays, that are connected to each other using parallel feeding.

1.5.4 Grating lobes

The grating lobe is defined as *"a lobe, other than the main lobe, produced by an array antenna when the inter-element spacing is sufficiently large to permit the in-phase addition of radiated fields in more than one direction."*[1].

That means when the spacing between elements of the array $d \geq \lambda_0/2$, multiple local maxima that have equal magnitude are generated. The greatest maximum is considered the main lobe, and the other local maxima are called grating lobes. [1]

2 Single patch antenna analysis

This chapter contains the analysis of single patch antennas comparing different feeding structures. The selected feeding structures are the following:

- Inset feeding technique
- Proximity feeding technique
- Aperture feeding technique

This chapter also contains the selection of the substrates upon which the single patch antennas and the subsequent 2x2 antenna array are to be analyzed. The analyzed patch antennas are implemented using the Ansys Electronic Desktop, specifically the Ansys HFSS.

2.1 Selection of substrates

In this section, the selection of the substrates is discussed.

2.1.1 Substrate comparison

For proper substrate selection several substrates were considered. The considered substrates can be seen in the table 2.1.

	RT/Duroid 5880	RT/Duroid 5870	RO3003	RO4003C	RO4350B	Unit
Dielectric constant	2.2	2.33	3	3.55	3.66	-
Dissipation factor 10 GHz	0,0009	0,0012	0,001	0,0027	0,0037	-
Volume resistivity	2×10^7	2×10^7	1×10^7	1.7×10^{10}	1.2×10^{10}	$M\Omega \times cm$
Surface resistivity	3×10^7	2×10^7	1×107	4.2×10^9	5.7×10^9	$M\Omega$
Substrate height:	0.127	0.127	0.13	0.203	0.101	mm
	0.254	0.254	0.25	0.305	0.168	mm
	0.381	0.381	0.5	0.406	0.254	mm
	0.508	0.508	0.75	0.508	0.338	mm
	0.787	0.787	1.52	0.813	0.422	mm
					0.508	mm
					0.762	mm

Tab. 2.1: Substrate parameters

2.1.2 Selected substrates

The selected substrates were the RT/Duroid 5880 and RO4350B from rogers corporation.

RT/Duroid 5880

Rogerscorp RT/Duroid 5880 hereinafter referred to as Duroid is a glass microfiber reinforced *Polytetrafluorethylen* (PTFE) composite. Thanks to the randomly oriented microfibers Duroid achieves exceptional dielectric constant uniformity. This uniformity is also achieved over wide frequency ranges and in addition, the Duroid has also a small dissipation factor. The values can be seen in the table 2.1.

The selected basic substrate height was $0.254mm$, this value was selected to prevent induction of additional modes by the 50Ω microstrip line. For that the selected substrate height needed to satisfy that $w < \lambda_0/10$, where w is the width of the microstrip line. Also there is limit for substrate thickness for the antenna itself this limits is $h/\lambda_0 < 0.3/(2\pi\sqrt{\epsilon_r})$.

RO4350B

Rogerscorp RO4350B is ceramic reinforced hydrocarbon composite laminate. Parameter wise they are worse than the Duroid, but they are still sufficient. The reason for selecting this substrate material was the fact that the board can be manufactured using standard *printed circuit board* (PCB) manufacturing methods, that are used for manufacturing FR-4 based PCBs. This results in lower manufacturing cost.

As with Duroid, the substrate height was selected to satisfy the $w < \lambda_0/10$ condition. Thanks to the higher ϵ_r a wider range of substrate heights could be chosen, but because the height of the Duroid substrate was selected as $0.254mm$, so this value was selected as well.

Prepregs

To implement a multilayer structure compatible prepregs were selected. For that, the selected prepregs were chosen with electrical properties as close as possible to the basic substrate. For the Duroid the Rogerscorp CuClad 6250 was selected and for the RO4350B, the Rogerscorp RO4450F was selected.

2.2 Single patch antennas on the Duroid substrate

This section focuses on the comparison of the different feeding techniques for single patch antennas on the RT/Duroid substrate.

2.2.1 Design parameters

Since the aperture-fed patch antenna and proximity-fed patch antenna require a multi-layer structure, the stackup has to be considered. Because it is assumed that the prepreg to be used with the Duroid is the Cuclad 6250 which has very close electric properties to the selected Duroid, the following stackups were selected. The thickness of the prepreg is $0.0381mm$ so for the aperture-fed patch, the core is layered with six prepregs. For the proximity-fed patch, the case considered is that 3 layers of prepregs between two cores of dimension $h = 0.127\ mm$. This gives approximately the same distance from the patch to the ground across all three implementations. The resulting selected distance between patch and ground is $254\mu m$.

First, the initial dimension W_p and L_p were calculated using equations 1.7 to 1.11 respectively. That gives for $W_p = 4.6472mm$ and for $L_p = 3.823mm$. These resulting values were taken as the initial dimensions of the patch antennas for all three feeding structures.

Example of calculation of patch antenna dimensions:

$$W_{\mathrm{P}} = \frac{3 \cdot 10^8}{2 \cdot 25.5 \cdot 10^9}\sqrt{\frac{2}{2.2+1}} = 4.647\,mm \tag{2.1}$$

$$\epsilon_{\mathrm{eff}} = \frac{2.2+1}{2} + \frac{2.2-1}{2}\left(\frac{1}{\sqrt{1+\frac{2\cdot 2.54\cdot 10^{-4}}{4.647\cdot 10^{-3}}}}\right) = 2.066 \tag{2.2}$$

$$L_{\mathrm{eff}} = \frac{3 \cdot 10^8}{2 \cdot 25.5 \cdot 10^9\sqrt{2.066}} = 4.089\,mm \tag{2.3}$$

$$\Delta L = 2.54 \cdot 10^{-4} \cdot 0.412 \cdot \frac{(2.066+0.3)\left(\frac{4.647\cdot 10^{-3}}{2.54\cdot 10^{-4}}+0.264\right)}{(2.066-0.258)\left(\frac{4.647\cdot 10^{-3}}{2.54\cdot 10^{-4}}+0.8\right)} = 0.133\,mm \tag{2.4}$$

$$L_p = L_{\mathrm{eff}} - 2\Delta L = 4.089 - 0.266 = 3.823\,mm \tag{2.5}$$

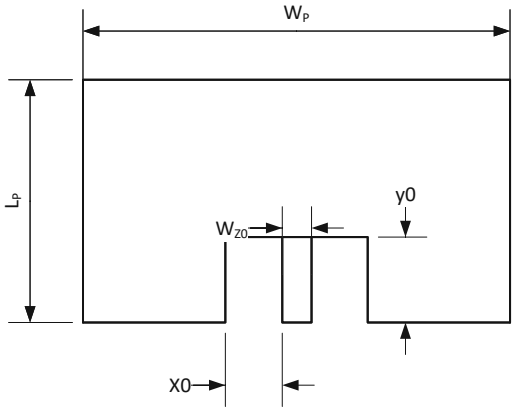

Fig. 2.1: Inset-fed patch

In figure 2.1 the dimensions of the inset-fed patch antenna can be seen. The initial position of the feeding point y_0 and x_0 are calculated using the equation 1.19 for y_0 and the $x_0 = W_{Z50}/2$, where the W_{Z50} is the width of the 50Ω feeding line.

Example of calculations:

$$G_1 = \frac{0.004647}{120\lambda_0}\left[1 - \frac{1}{24}(534.44 \cdot 0.000254)^2\right] = 0.00329 \tag{2.6}$$

$$R_{\text{in}} = \frac{1}{2G_1} = \frac{1}{2 \cdot 0.00329} = 151.91\,\Omega \tag{2.7}$$

$$y_0 = \frac{3.823}{\pi}\arccos\left(\sqrt{\frac{50}{151.91}}\right) = 1.168\,mm \tag{2.8}$$

$$B = \frac{59.95\pi^2}{50 \cdot \sqrt{2.2}} = 7.9422 \tag{2.9}$$

$$\frac{W_{Z50}}{h} = \frac{2}{\pi}[(B-1) - \ln(2B-1)] + \frac{(2.22-1)}{\pi \cdot 2.22}[\ln(2B-1) + 0.293 - \frac{0.517}{2.22}] = 3.1834 \tag{2.10}$$

$$W_{Z50} = 3.1834 * 0.000254 = 0.808\,mm \tag{2.11}$$

	Initial	After Optimization	Unit
W_P	4.647	4.6472	mm
L_P	3.823	3.838	mm
y_0	1.168	1.120	mm
x_0	0.404	0.3915	mm

Tab. 2.2: Dimensions of inset-fed patch on duroid substrate

As can be seen in table 2.2 the resulting dimensions after optimization for the inset-fed patch antenna are very close to the calculated ones.

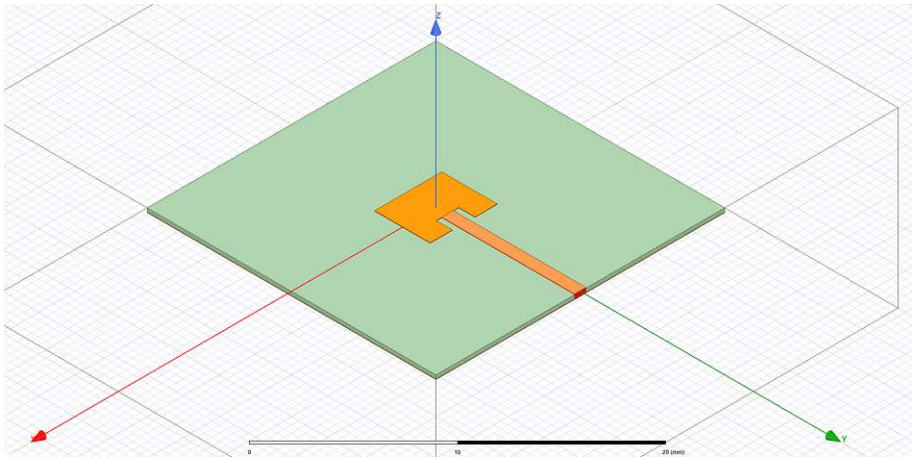

Fig. 2.2: Inset-fed patch HFSS model

In figure 2.2, the HFSS model of the inset-fed patch antenna can be seen. The length of the patch antenna runs along the y-axis and the width of the patch antenna runs along the x-axis. The broadside of the patch is along the z-axis. The port is represented by the red rectangle.

Proximity-fed patch antenna

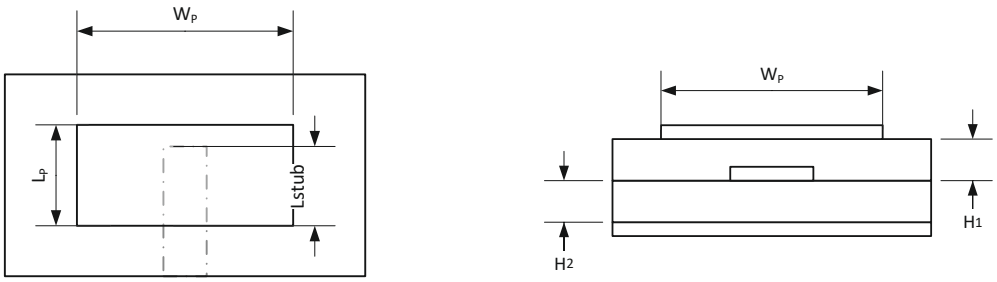

(a) Top view (b) Side view

Fig. 2.3: Proximity-fed patch

	Initial	After Optimization	Unit
Wp	4.647	4.6472	mm
Lp	3.823	3.388	mm
L_{stub}	1.9	0.894	mm
H_1	0.127	0.127	mm
H_2	0.1143	0.1143	mm

Tab. 2.3: Dimensions of proximity-fed patch on duroid substrate

For the proximity-fed patch antenna, the initial L_{stub} was taken in the middle of the patch and then optimized for good impedance matching. The initial and resulting dimensions can be seen in the table2.3.

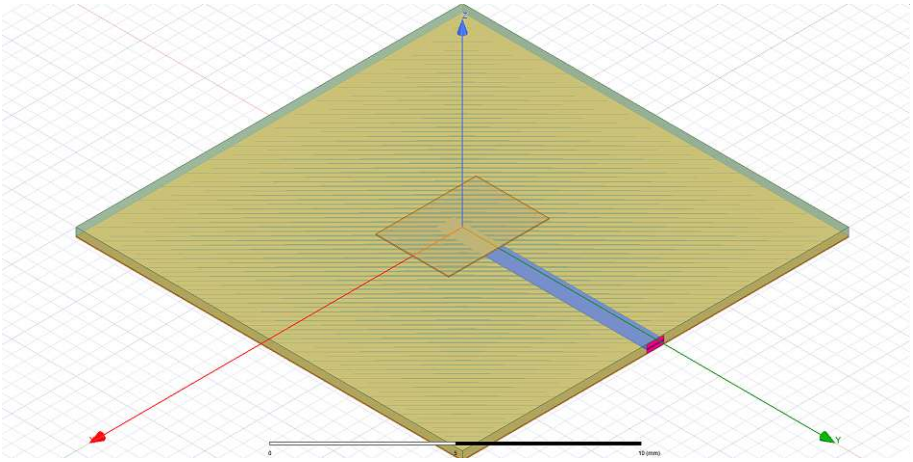

Fig. 2.4: Proximity-fed patch HFSS model

In figure 2.4, the HFSS model of the inset-fed patch antenna can be seen. The length of the patch antenna runs along the y-axis and the width of the patch antenna runs along the x-axis. The broadside of the patch is along the z-axis. The port is represented by the purple rectangle.

Aperture-fed patch antenna

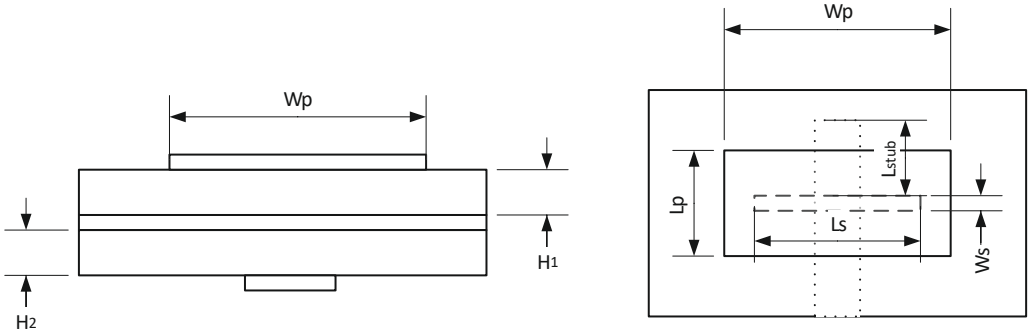

Fig. 2.5: Aperture-fed patch

	Initial	After Optimization	
W_p	4.6472	4.6472	mm
L_p	3.823	3.395	mm
L_s	1.15	1.864	mm
W_s	0.115	0.18640	mm
L_{stub}	2.323	1.983	mm
H_1	0.254	0.254	mm
H_2	0.254	0.254	mm

Tab. 2.4: Dimensions of aperture-fed patch on duroid substrate

For the aperture fed patch antenna the initial width of the slot was taken as $0.1\lambda_0$ and then optimized for good matching.

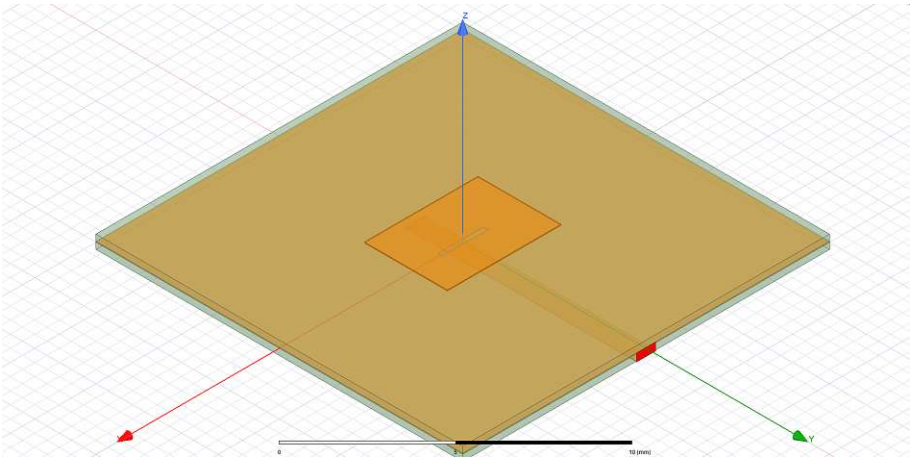

Fig. 2.6: Proximity-fed patch HFSS model

In figure 2.6, the HFSS model of the inset-fed patch antenna can be seen. The length of the patch antenna runs along the y-axis and the width of the patch antenna runs along the x-axis. The broadside of the patch is along the z-axis. The port is represented by the red rectangle.

2.2.2 Performance comparison

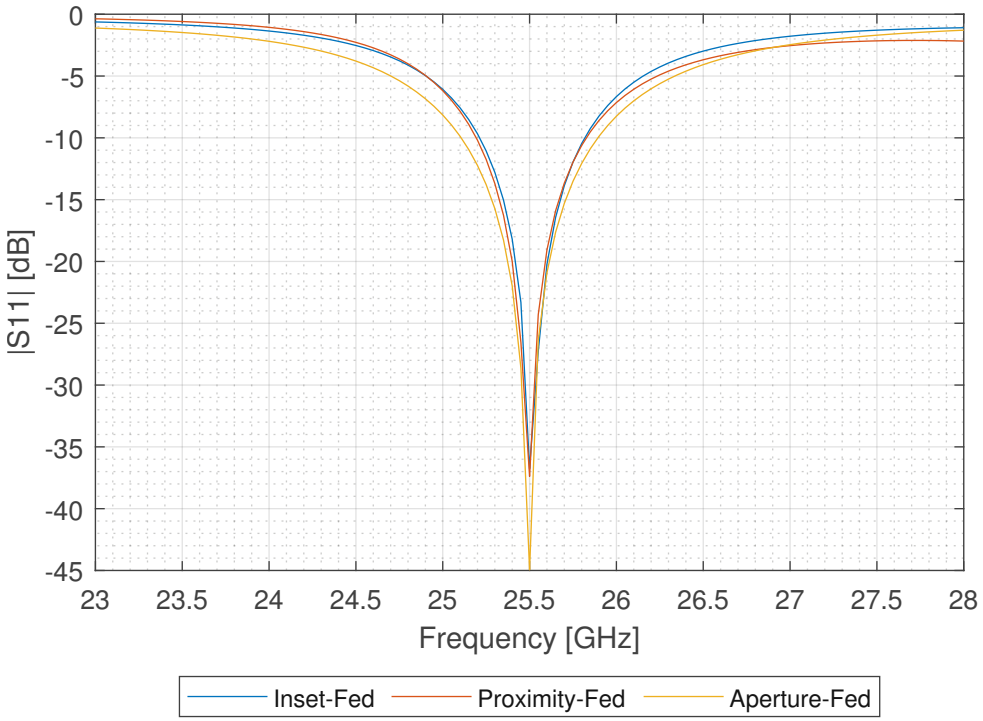

Fig. 2.7: $|\ S_{11}\ |$ of single patches on Duroid substrate

In figure 2.7 there are three lines each representing one of the feeding techniques. From these the bandwidth can be calculated for $\mid S_{11} \mid \leq -10dB$ using the frequencies listed in the table 2.5:

	Inset-fed	Proximity-fed	Aperture-fed
F_{Lower}	25.212 GHz	25.191 GHz	25.105 GHz
F_{Upper}	25.819 GHz	25.829 GHz	25.893 GHz
BW	607 MHz	638 MHz	788 MHz

Tab. 2.5: $\mid S_{1,1} \mid$ frequency limits of the patches on Duroid substrate

For the inset-fed patch antenna the bandwidth is $BW = 607\ MHz$, for the proximity-fed patch antenna the bandwidth is $BW = 638\ MHz$ and for the aperture fed patch antenna the bandwidth is $BW = 788\ MHz$. Also the optimization was done in relation to the $\mid S_{11} \mid$.

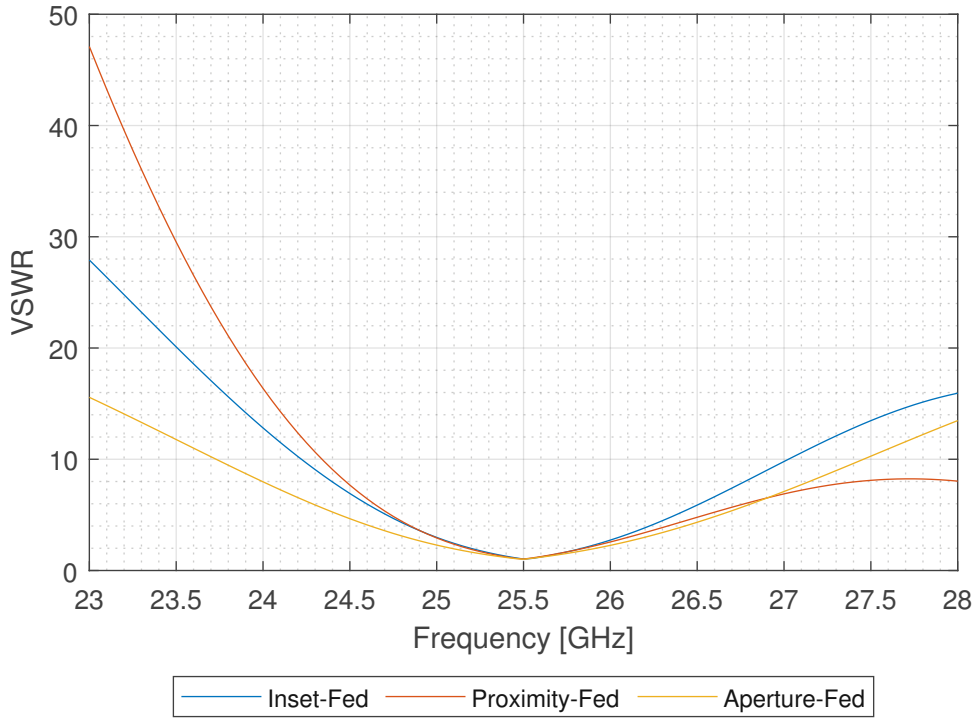

Fig. 2.8: VSWR of single patches on Duroid substrate

Bandwidth can also be calculated from the VSWR. The VSWR can be seen in the figure 2.8, the bandwidth of VSWR is taken for the value of $VSWR \leq 2$, which corresponds to $\mid S_{11} \mid \leq -9.542dB$.

	Inset-fed	Proximity-fed	Aperture-fed
$\text{VSWR}_{\text{Lower}}$	25.2 GHz	25.175 GHz	25.08 GHz
$\text{VSWR}_{\text{Upper}}$	25.835 GHz	25.85 GHz	25.92 GHz
BW	635 MHz	675 MHz	900 MHz

Tab. 2.6: VSWR frequency limits for single patch antennas on Duroid substrate

From the table 2.6, the bandwidth is calculated. For the inset-fed patch antenna the bandwidth was $BW = 635\ MHz$, for the proximity-fed patch antenna the bandwidth was $BW = 675\ MHz$ and for the aperture fed patch antenna the bandwidth of $BW = 900\ MHz$.

Based on the case of $\mid S_{1,1} \mid$ and VSWR the antenna with the largest bandwidth is the aperture-fed antenna, and the worst performs the inset-fed patch antenna. The bandwidth of the proximity-fed patch antenna, gives only 75% of aperture-fed antenna's bandwidth. The inset-fed gives only 70.6%.

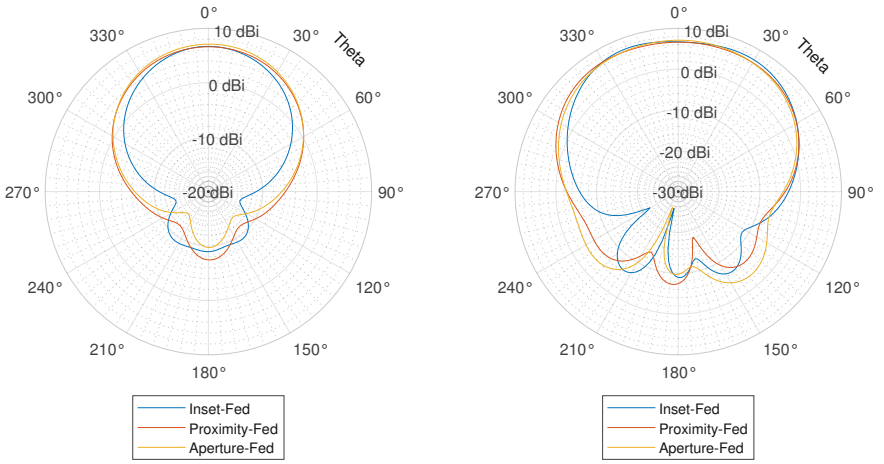

(a) $\Phi = 0°$ (b) $\Phi = 90°$

Fig. 2.9: Co-polarized component of realized gain of Duroid single patches

From the graphs of the co-polarized component realized gain, we can see that in the $\Phi = 90°$ plane the Aperture-fed patch antenna exhibits the largest amount of the backward radiation. This radiation is not directed directly backward $\theta = 180°$, but backward sideways. The largest direct backward radiation exhibits the proximity-fed patch antenna.

	Inset-fed	Proximity-fed	Aperture-fed
$G_{\mathrm{re,max}}\ for\ \Phi = 0°$	6.68 dBi	6.61 dBi	7.09 dBi
$G_{\mathrm{re,max}}\ for\ \Phi = 90°$	7.27 dBi	6.72 dBi	7.09 dBi
$FBR\ for\ \Phi = 0°$	15.6 dB	14 dB	16.9 dB
$FBR\ for\ \Phi = 90°$	15.64 dB	14 dB	16.82 dB

Tab. 2.7: Maximum realized gain and front to back ratio of the single patch antennas on duroid substrate

Table 2.7 shows the values of maximum realized gain and the front to back ratio. For $\phi = 0°$ plane the largest gain exhibits the aperture-fed patch antenna. For $\phi = 90°$ plane, the largest gain exhibits the inset-fed patch antenna. Unlike with the case for $\phi = 0°$, the peak gain isn't at $\theta = 0°$, but at $\theta = 340°$. Best front to back ratio exhibits the aperture-fed patch for both the $\phi = 0°$ and the $\phi = 90°$ planes.

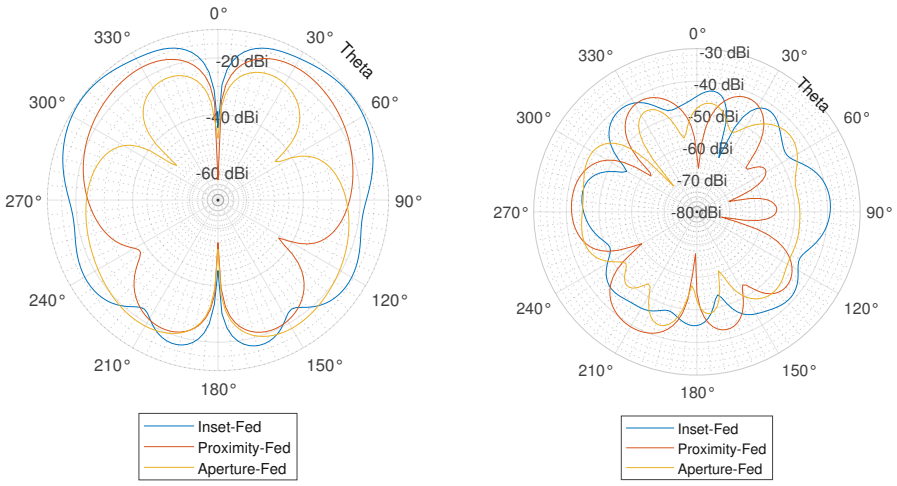

(a) $\Phi = 0°$ (b) $\Phi = 90°$

Fig. 2.10: Cross-polarized component of realized gain of Duroid single patches

From the cross-polarized component of the realized gain pattern, it can be seen that the highest gain has the inset-fed patch antenna. It can be also seen that the aperture-fed patch antenna in the direction desired broadside radiation has the smallest gain of the cross polarized component. These facts can be better seen in the cross polarization ratio.

	Inset-fed	Proximity-fed	Aperture-fed
$\Phi = 0°$	68°	84°	80°
$\Phi = 90°$	106°	122°	110°

Tab. 2.8: Half-power beam-width of patch antennas on Duroid substrate

The table 2.8 lists the half-power beam-width of the total realized gain. The tightest beam is generated by the inset-fed patch antenna and the widest beam is generated by the proximity fed patch antenna.

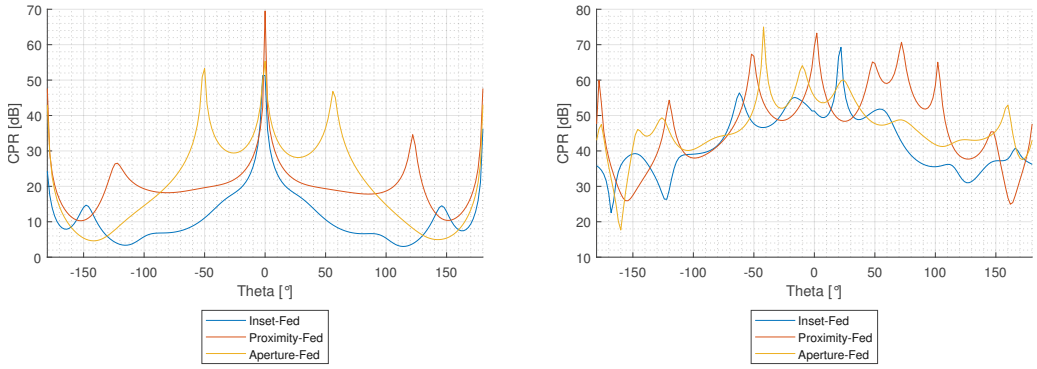

(a) $\Phi = 0°$ (b) $\Phi = 90°$

Fig. 2.11: Cross polarization ratio of single patches on Duroid substrate

For $\phi = 0°$ plane, the inset-fed patch antenna has a cross polarization ratio of 51.28 dB at $\theta = 0°$, the proximity-fed patch antenna has 69.495 dB and the aperture-fed patch antenna 55.34 dB.

Over the half-power beam-width for $\Phi = 0°$ the cross polarization ratio of the inset-fed patch antenna gradually degrades to 15.6 dB, for the proximity fed patch antenna this degrades to 19.8 dB and for the aperture-fed patch antenna it degrades and rises again over the half-power beam-width with the minimum being 28.1 dB.

For $\Phi = 90°$ the the inset fed patch antenna holds above 46.6 dB, proximity patch antenna holds above 47.7 dB, and the aperture-fed patch antenna holds above 47.45 dB.

On average, over the beam-width angle, the aperture-fed patch antenna performs best in respect of the cross polarization ratio.

Frequency	25 GHz	25.25 GHz	25.5 GHz	25.75 GHz	26 GHz
Inset-fed	5.935 dBi	6.865 dBi	7.234 dBi	7.125 dBi	6.501 dBi
Proximity-fed	5.538 dBi	6.452 dBi	6.794 dBi	6.547 dBi	5.942 dBi
Slot-fed	6.577 dBi	7.023 dBi	7.121 dBi	6.844 dBi	6.273 dBi

Tab. 2.9: Peak realized gain over frequency on Duroid substrate

As can be seen in the table 2.9, over the frequency band, the inset-fed patch antenna exhibits the highest peak realized gain. The inset-fed patch antenna has also the smallest variation of the gain over the frequency band.

Frequency	25 GHz	25.25 GHz	25.5 GHz	25.75 GHz	26 GHz
Inset-fed	0.926	0.935	0.938	0.936	0.929
Proximity-fed	0.932	0.943	0.953	0.961	0.967
Aperture-fed	0.945	0.951	0.955	0.956	0.955

Tab. 2.10: Antenna efficiency over frequency on Duroid substrate

In the table 2.19, the efficiency over frequency of the patch antennas can be seen. The efficiency of the antenna is best for the aperture-fed patch antenna. The second best is the proximity-fed patch antenna.

2.3 Single patch antennas on the RO4350B substrate

This section focuses on the comparison of the different feeding techniques for single patch antennas on the RO4350B substrate.

2.3.1 Design Parameters

As with the antennas realized on RT/Duroid, the proximity-fed and aperture-fed patch antenna are multi-layer structures. The case considered for the aperture-fed patch antenna is that two layers of the RO4450F prepreg are used together with a core layer of RO4350B. The case considered for proximity fed patch antenna is the following two layers of prepregs used together with the core of height $h = 168\ mm$.

The initial and optimized dimensions of the patch antennas are listed in the tables 2.11,2.12 and 2.13.

	Initial	After Optimization	
Wp	3.851	3.854	mm
Lp	2.985	2.979	mm
y0	0.970	0.964	mm
x0	0.278	0.278	mm

Tab. 2.11: Dimensions of inset-fed patch on RO4350B substrate

	Initial	After Optimization	
Wp	3.851	3.897	mm
Lp	2.918	2.833	mm
L_stub	1.492	2.074	mm
H_1	0.168	0.168	mm
H_2	0.204	0.204	mm

Tab. 2.12: Dimensions of proximity-fed patch on RO4350B substrate

	Initial	After Optimization	
Wp	3.851	3.8509	mm
Lp	2.985	2.6350	mm
Ls	1.5	1.6776	mm
Ws	0.15	0.1677	mm
L_stub	1.925	1.7557	mm
H_1	0.254	0.254	mm
H_2	0.204	0.204	mm

Tab. 2.13: Dimensions of aperture-fed patch on RO4350B substrate

2.3.2 Performance comparison

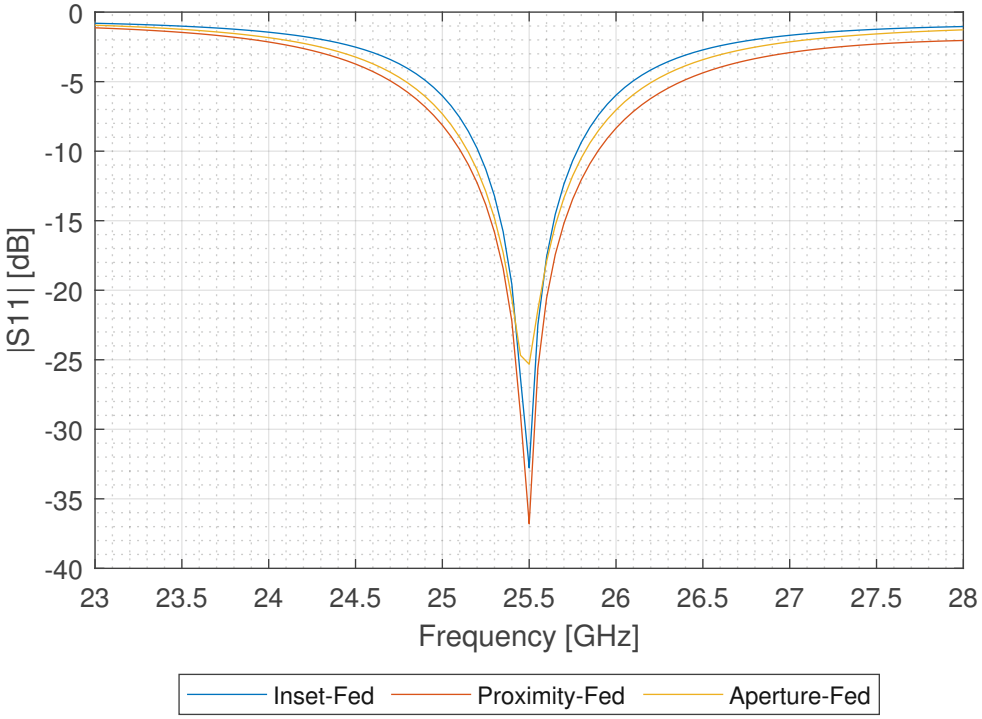

Fig. 2.12: $|\ S_{11}\ |$ of single patches on RO4350 substrate

	Inset-fed	Proximity-fed	Aperture-fed
F_{Lower}	25.206 GHz	25.105 GHz	25.147 GHz
F_{Upper}	25.776 GHz	25.896 GHz	25.822 GHz
BW	576 MHz	791 MHz	675 MHz

Tab. 2.14: $|\ S_{11}\ |$ frequency limits of the patches on RO4350B substrate

In table 2.14, the upper and lower frequency limits of $S_{11} \leq -10\ dB$ can be seen. From these frequencies, the bandwidths of the patch antennas can be calculated. For the inset-fed patch antenna, the bandwidth is $BW = 576\ MHz$, for the proximity-fed patch antenna the bandwidth is $BW = 791\ MHz$ and for the aperture-fed patch antenna the bandwidth is $BW = 675\ MHz$. The bandwidth of the proximity-fed patch antenna is the highest. This is caused by the fact that the height of the patch from the ground is higher than for the other two cases. This is caused by the fact that the selected height of the substrate was based on real substrate materials.

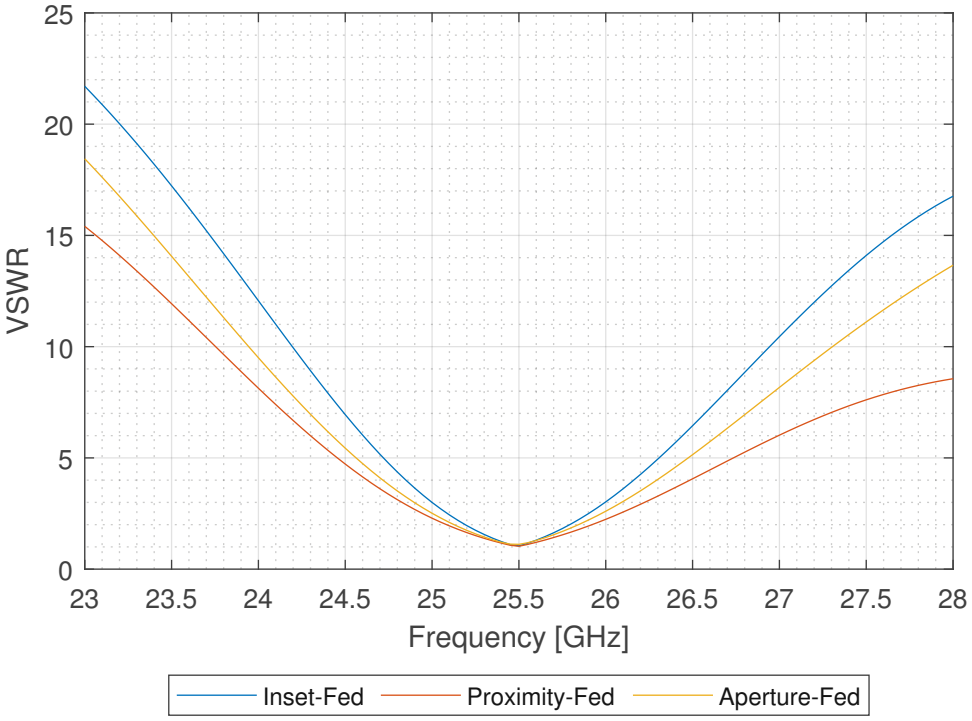

Fig. 2.13: VSWR of single patches on RO4350 substrate

The VSWR can be seen in figure 2.13. As in the case of the patch antennas on the Duroid substrate, the bandwidth of VSWR is taken for the value of $VSWR \leq 2$. For the value $VSWR = 2$, we take the upper and lower frequency limits, and these can be seen in the table 2.15.

	Inset-fed	Proximity-fed	Aperture-fed
$\text{VSWR}_{\text{Lower}}$	25.189 GHz	25.0831 GHz	25.148 GHz
$\text{VSWR}_{\text{Upper}}$	25.793 GHz	25.9233 GHz	25.850 GHz
BW	604 MHz	840 MHz	702 MHz

Tab. 2.15: VSWR frequency limits of the patches on RO4350B substrate

For the inset-fed patch antenna, the bandwidth is $BW = 604\ MHz$, for the proximity-fed patch antenna, the bandwidth is $BW = 840\ MHz$, and for the aperture-fed patch antenna, we get the bandwidth of $BW = 702\ MHz$.

Based on the case of $\mid S_{1,1} \mid$ and VSWR the antenna with the largest bandwidth is the proximity-fed antenna, and the worst performs the inset-fed patch antenna. The bandwidth of the aperture-fed patch antenna, gives only 83.6% of aperture-fed antenna's bandwidth. The inset-fed gives only 71.9%.

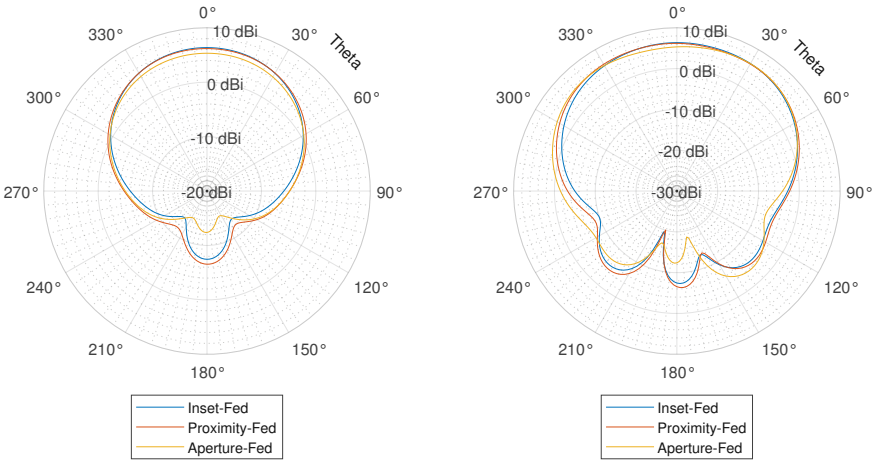

(a) $\Phi = 0°$ (b) $\Phi = 90°$

Fig. 2.14: Co-polarized component of realized gain of RO4350 single patches

In the $\Phi = 0°$ plane, the gain in the broadside direction $\theta = 0°$ is the largest for the inset-fed patch with 6.35 dBi, second is the proximity-fed patch antenna with 6.18 dBi and the last is the aperture-fed patch antenna with 5.31 dBi. In the $\Phi = 90°$ plane the gain at $\theta = 0°$ is same, but the aperture-fed patch antenna exhibits a peak at $\theta = 30°$ with 6.03 dBi. We can also see that at $\Phi = 0°$ the aperture coupled patch antenna exhibits the least amount of backward radiation, which can also be said for the $\Phi = 90°$ case. On the other hand, the aperture-fed patch antenna exhibits the largest side lobe at $\theta = 140°$

	Inset-fed	Proximity-fed	Aperture-fed
$G_{\mathrm{re,max}}\ for\ \Phi = 0°$	6.35 dBi	6.18 dBi	5.31 dBi
$G_{\mathrm{re,max}}\ for\ \Phi = 90°$	6.35 dBi	6.18 dBi	6.03 dBi
$FBR\ for\ \Phi = 0°$	13.8 dB	12.7 dB	17.7 dB
$FBR\ for\ \Phi = 90°$	14.1 dB	12.5 dB	17.7 dB

Tab. 2.16: Maximum realized gain and front to back ratio of the single patch antennas on RO4350 substrate

Table 2.16 shows that the best front to back ratio exhibits the aperture-fed patch antenna. This is valid for both the $\phi = 0°$ and the $\phi = 90°$ planes.

	Inset-fed	Proximity-fed	Aperture-fed
$\Phi = 0°$	88°	96°	98°
$\Phi = 90°$	112°	124°	130°

Tab. 2.17: Half-power beam-width of single patches at RO4350

In table 2.17 we can see that the half-power beam-widths of the antennas. The tightest beam has the inset-fed patch antenna and the broadest the aperture-fed patch antenna.

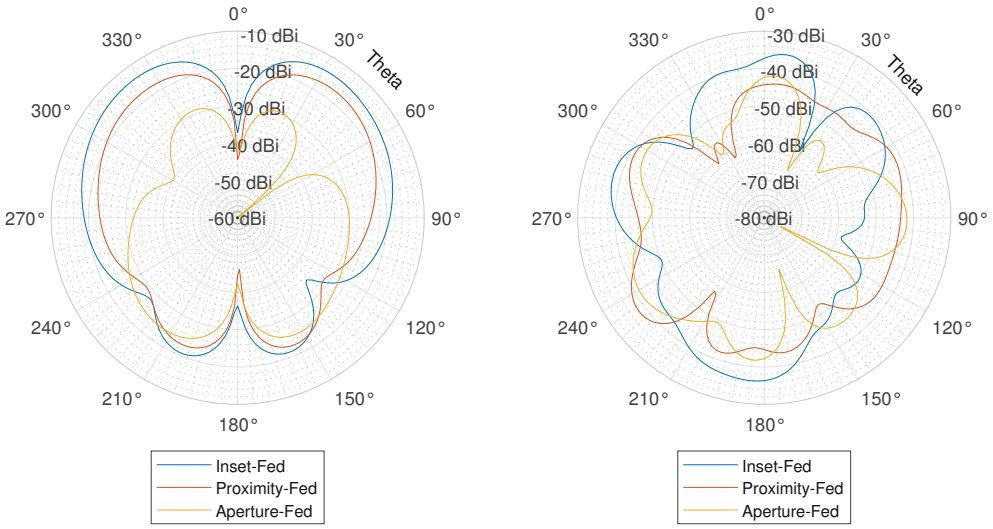

(a) $\Phi = 0°$ (b) $\Phi = 90°$

Fig. 2.15: Cross-polarized component of realized gain of RO4350 single patches

From the cross polarized component of the realized gain, it can be seen that the aperture-fed patch antenna has the smallest radiation pattern of all in the $\Phi = 0°$ plane, second best is the proximity-fed antenna, and worst is the inset-fed patch antenna. For the $\Phi = 90°$ plane in the direct broadside direction $\theta = 0°$ best is the proximity-fed. However, over the width of their respective beam-width, the aperture-fed patch antenna performs better.

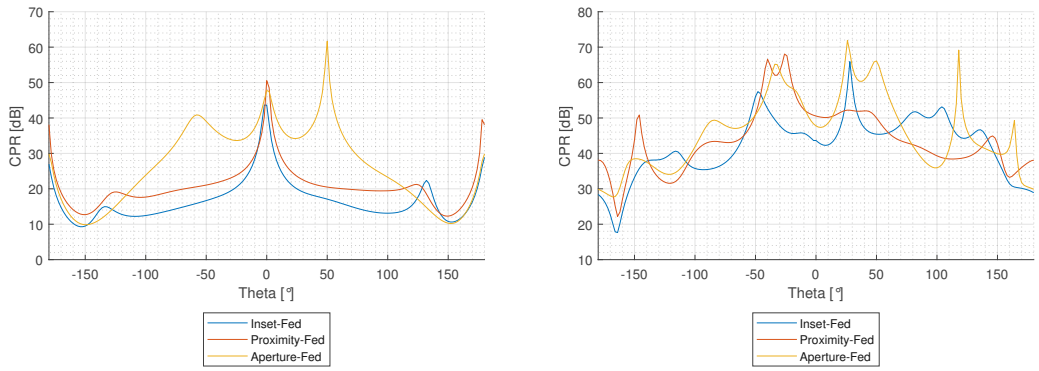

(a) $\Phi = 0°$ (b) $\Phi = 90°$

Fig. 2.16: Cross polarization ratio of single patches on RO4350 substrate

From the cross polarization ratio, we can see that for $\Phi = 0°$, the aperture-fed patch antenna exhibits the best cross polarization ratio across the width of its beam and the inset-fed patch antenna has the worst case.

Frequency	25 GHz	25.25 GHz	25.5 GHz	25.75 GHz	26 GHz
Inset-fed	5.256 dB	6.203 dB	6.462 dB	5.909 dB	5.835 dB
Proximity-fed	5.522 dB	6.028 dB	6.148 dB	5.867 dB	5.309 dB
Aperture-fed	4.917 dB	5.731 dB	6.037 dB	5.773 dB	5.073 dB

Tab. 2.18: Peak realized gain over frequency on RO4350B substrate

Table 2.18 shows that best peak realized gain at the center frequency exhibits the inset-fed patch antenna. The smallest variation over the frequency exhibits the proximity-fed patch antenna. The largest variation the aperture-fed patch antenna.

2.3.3 Antenna efficiency

Frequency	25 GHz	25.25 GHz	25.5 GHz	25.75 GHz	26 GHz
Inset-fed	0.814	0.829	0.834	0.830	0.816
Proximity-fed	0.873	0.88	0.883	0.881	0.876
Aperture-fed	0.818	0.835	0.842	0.840	0.827

Tab. 2.19: Antenna efficiency over frequency on RO4350B substrate

In table 2.19 the efficiencies over the frequency of the patch antennas can be seen. The best performance exhibits the proximity-fed patch antenna, second best is shown

by the aperture-fed patch antenna. The worst performance exhibits the inset-fed patch antenna.

3 Comparison of arrays with single element antennas

This chapter focuses on the comparison of the single patch antenna with simulated patch antenna array.

3.1 Common feeding structure

The array feeding structure was designed using parallel feeding. The patches themselves are fed by the 100Ω line. The discussed simulation designs are fed by an internal port.

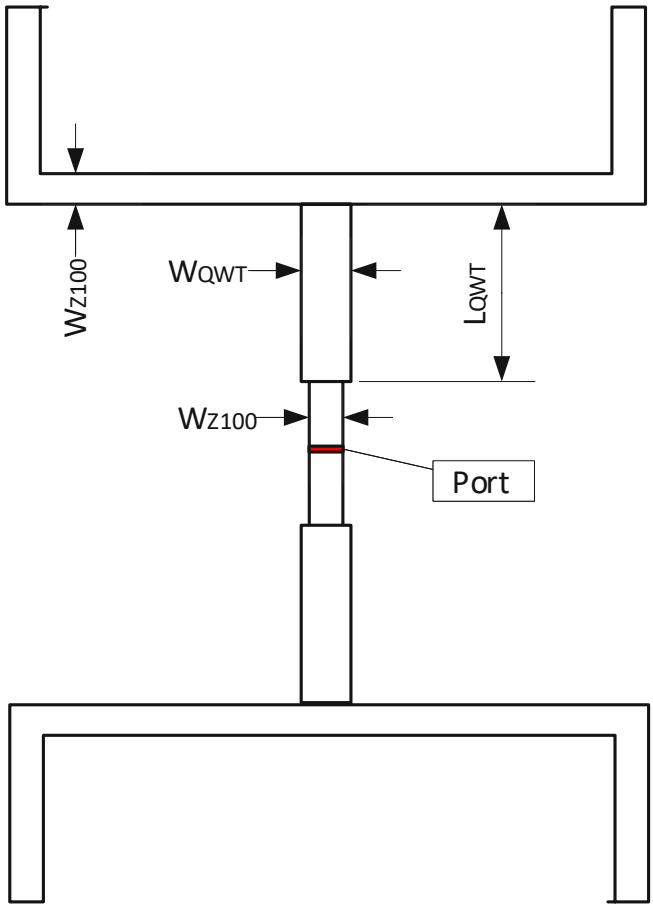

Fig. 3.1: Common feeding structure

Figure 3.1, shows the common feeding structure for all patch antenna arrays.

	Inset-fed Duroid	Inset-fed RO4350	Proximity-fed Duroid	Proximity-fed RO4350	Aperture-fed Duroid	Aperture-fed RO4350
W_{Z100}	0.228 mm	0.111 mm	0.189 mm	0.135 mm	0.228 mm	0.111 mm
W_{QWT}	0.449 mm	0.24 mm	0.430 mm	0.373 mm	0.449 mm	0.24 mm
L_{QWT}	2.183 mm	1.78 mm	2.183 mm	1.78 mm	2.183 mm	1.78 mm

Tab. 3.1: Dimensions of the common feeding structure

In table 3.1 the dimensions of the common feeding structure are listed. The W_{Z100} is the width of the 100 Ω line, the W_{QWT} is the width of the quarter-wave impedance transformer, and the L_{QWT} is the length of the quarter-wave impedance transformer, which is $L_{QWT} = \lambda_g/4$, where the λ_g is the guided wavelength in PCB substrate.

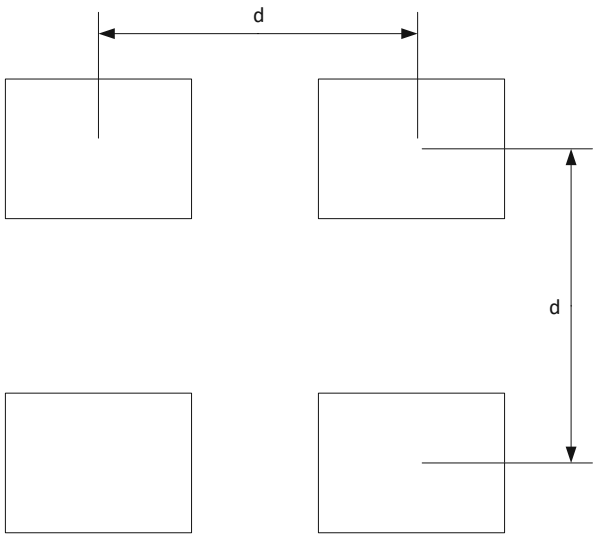

Fig. 3.2: 2x2 Array spacing

As shown in figure 3.2, the single elements of the antenna arrays are separated by distance d from each other. For this comparison, the spacing of the elements was chosen as $d = 0.72\lambda_0$. This distance was selected as a compromise between the level of grating lobes, the width of the beam, and to minimize the effects of the mutual coupling of the antennas, which adversely affects the radiation pattern and matching.

3.2 Inset-fed antennas on Duroid substrate

In this section, the single inset-fed patch antenna is compared to the simulated array, and the expected results acquired by the pattern multiplication with the array factor. These antennas are simulated on the Duroid PCB substrate. The array factor function is generated internally by the Ansys HFSS simulator. For 2x2 antenna array the peak value of the array factor function should be $6dB$, which mean that the peak gain of the resulting array should be $6dB$ higher than the peak gain of single patch antenna.

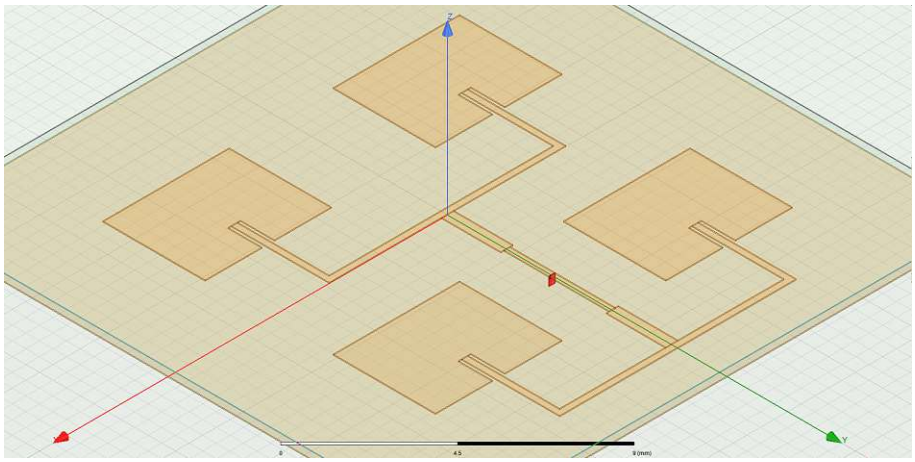

Fig. 3.3: HFSS model of the inset-fed patch antenna array

In figure 3.3 the HFSS model of the aperture-fed patch antenna array is illustrated. In the model the red rectangle in the middle of the feeding structure is the input port.

Dimension	Single Patch	Array	Unit
W_p	4.647	4.647	mm
L_p	3.838	3.759	mm
y_0	1.120	1.249	mm
x_0	0.3915	0.114	mm

Tab. 3.2: Dimensions of the inset-fed patch antennas on Duroid substrate

The extension to a 2x2 array required that the common feeding structure is matched to the patch antennas. The values for the individual inset-fed patch antennas after reoptimization can be seen in table 3.2.

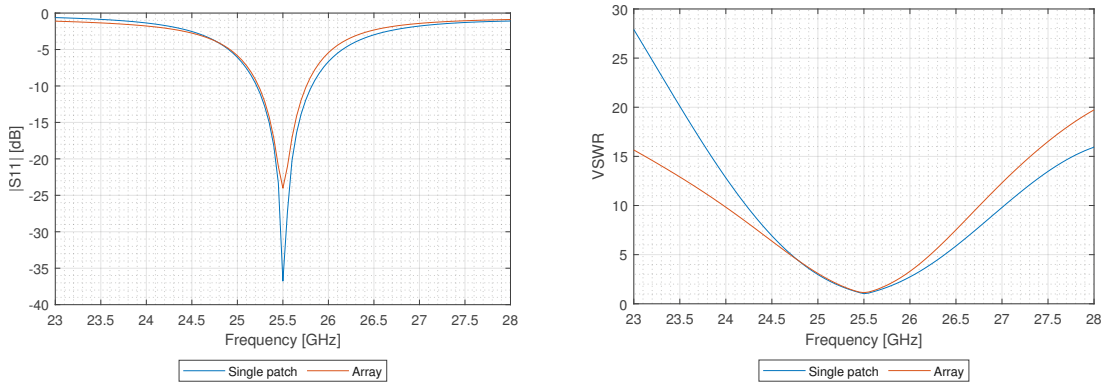

(a) $|\ S_{11}\ |$ (b) VSWR

Fig. 3.4: $|\ S_{11}\ |$ and VSWR of the inset-fed antenna on Duroid substrate

From the graphs, it can be seen that the rise of VSWR for the antenna array becomes steeper. This results in a smaller frequency bandwidth than with the single element patch antenna.

Dimension	Single Patch	Array	Unit
$\|\ S_{11}\ \|_{\text{Upper}}$	25.819	25.760	GHz
$\|\ S_{11}\ \|_{\text{Lower}}$	25.212	25.233	GHz
$VSWR_{\text{Upper}}$	25.835	25.774	GHz
$VSWR_{\text{Lower}}$	25.2	25.215	GHz
BW_{S11}	602	527	GHz

The $S_{1,1}$ bandwidth of single element patch antenna is 602 MHz and the bandwidth of the 2x2 array is 527 MHz that is 75 MHz decrease or about 12.5 %

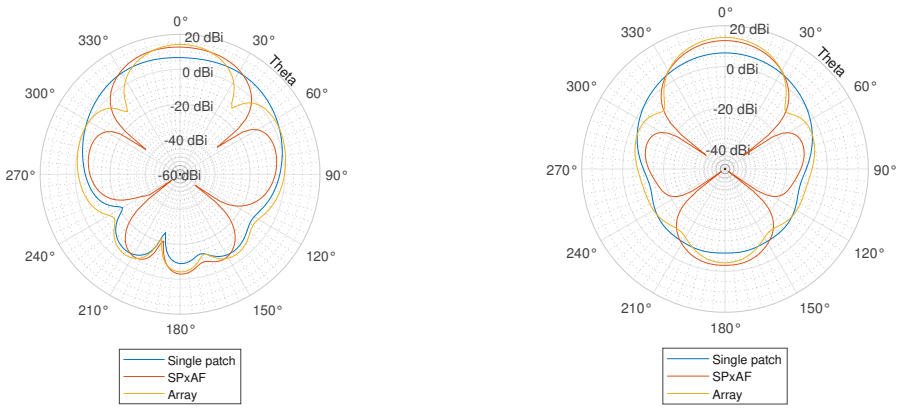

(a) $\Phi = 90°$ (b) $\Phi = 0°$

Fig. 3.5: Total realized gain of the inset-fed antenna on Duroid substrate

Figure 3.5 shows that the expected pattern created by pattern multiplication with array factro function varies from the pattern of the simulated array. On one hand the pattern is tighter, but on the other hand, the magnitude of the grating lobe is higher.

	Singele patch	Array factor	Simulated array
$G_{\text{re,max}}$	6.68 dBi	12.7 dBi	14.2 dBi
$G_{\text{re,grating}}$	N/A	-9.8 dB	-4 dB
$G_{\text{re,back}}$	-8.96 dB	-2.94 dB	-4.17 dB

Tab. 3.3: Peak, grating lobe peak, back lobe total realized gain for inset-fed array on Duroid substrate for $\Phi = 0°$

In table 3.3 and hereafter, $G_{\text{re,grating}}$ stands for peak realized gain of the grating lobe, and $G_{\text{re,back}}$ stands for peak realized gain of back lobe.

	Singele patch	Array factor	Simulated array
$G_{\text{re,max}}$	7.27 dBi	12.7 dBi	14.2 dBi
$G_{\text{re,grating}}$	N/A	-3.8 dB	2.5 dB
$G_{\text{re,back}}$	-8.96 dB	-3.28 dB	-4.17 dB

Tab. 3.4: Peak, grating lobe peak, back lobe total realized gain for inset-fed array on Duroid substrate for $\Phi = 90°$

Tables 3.3 and 3.4 show that the magnitude of the realized gain in the broadside direction $\theta = 0°$ is higher 14.2 dBi, instead of 12.7 dBi expected by pattern multiplication.

The magnitude of grating lobe is about -4 dBi when pattern multiplication predicted about -9.8 dBi for $\phi = 0°$ plane and for $\phi = 90°$ plane the side lobe is 2.5 dBi when pattern multiplication predicted -3.8 dBi.

With those the *Side lobe level* (SLL) can be calculated,which is the difference between side-lobe, in this case the gratin lobe ,and main lobe. The SLL is 18.2 dB for $\phi = 0$ and $SLL = 11.7$ dB for $\phi = 90$.

These are bellow the levels predicted by pattern multiplication, which are $SLL = 22.64$ dB for $\phi = 0°$ and $SLL = 16.5$ dB for $\phi = 90°$.

	Single Patch	Array factor	Array
$\Phi = 0°$	68°	40°	36°
$\Phi = 90°$	106°	52°	32°

Tab. 3.5: Half-power beam-width of the inset-fed antenna on Duroid substrate

The table 3.5 shows that the resulting half-power beam-width of the array is tighter than expected by pattern multiplication with array factor.

3.3 Proximity-fed antennas on Duroid substrate

In this section, the proximity-fed patch antenna is compared to the simulated array, and the expected results acquired by the pattern multiplication with the array factor. These antennas are realized on the Duroid PCB substrate.

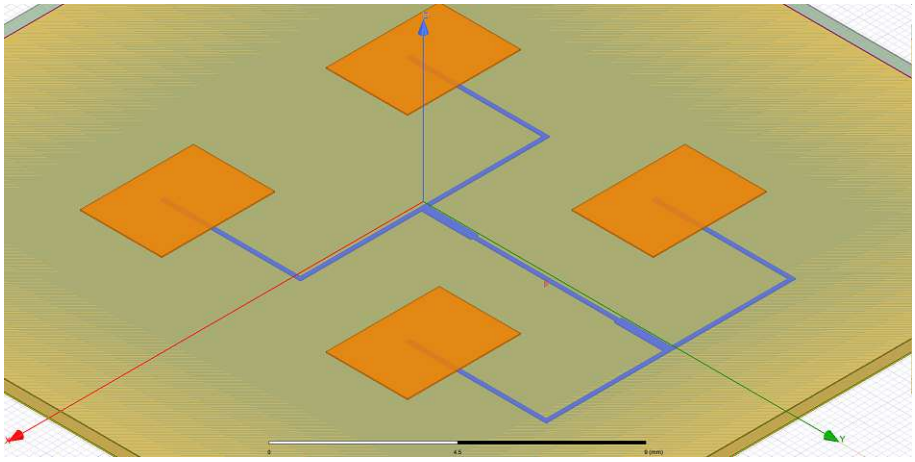

Fig. 3.6: HFSS model of the proximity-fed patch antenna array

Figure 3.6 shows the HFSS model of the aperture-fed patch antenna array. In the model the purple rectangle in the middle of the feeding structure is the input port.

Dimension	Single Patch	Array	Unit
W_p	4.647	4.647	mm
L_p	3.388	3.693	mm
L_{stub}	0.894	1.850	mm
H_1	0.127	0.127	mm
H_2	0.1143	0.1143	mm

Tab. 3.6: Dimensions of proximity-fed patch antennas on Duroid substrate

The extension to a 2x2 array required that the common feeding structure is matched to the patch antennas. The values for the individual proximity-fed patch antennas after reoptimization can be seen in table 3.6.

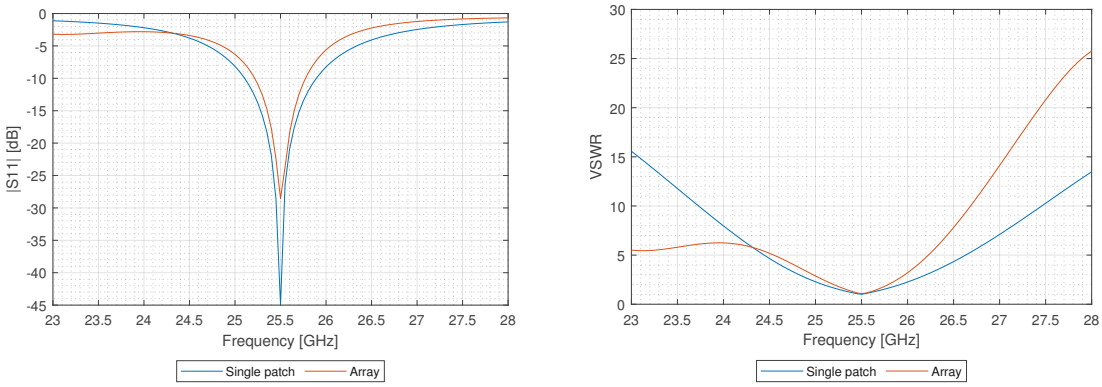

(a) $\mid S_{11} \mid$ (b) VSWR

Fig. 3.7: $\mid S_{11} \mid$ and VSWR of the proximity-fed antenna on Duroid substrate

Dimension	Single Patch	Array	Unit
$\mid S_{11} \mid_{\text{Upper}}$	25.829	25.8	GHz
$\mid S_{11} \mid_{\text{Lower}}$	25.191	25.2	GHz
$VSWR_{\text{Upper}}$	25.85	25.821	GHz
$VSWR_{\text{Lower}}$	25.175	25.170	GHz
BW	639	600	MHz

Tab. 3.7: Frequency limits of the proximity-fed antenna on Duroid substrate

From table 3.7 the bandwidth can be calculated for the cases of the single patch and the resulting array. The bandwidth for the single patch is $BW = 639\ MHz$ and for the resulting 2x2 array the bandwidth is $BW = 600MHz$, that is a 39 MHz decrease of the bandwidth.

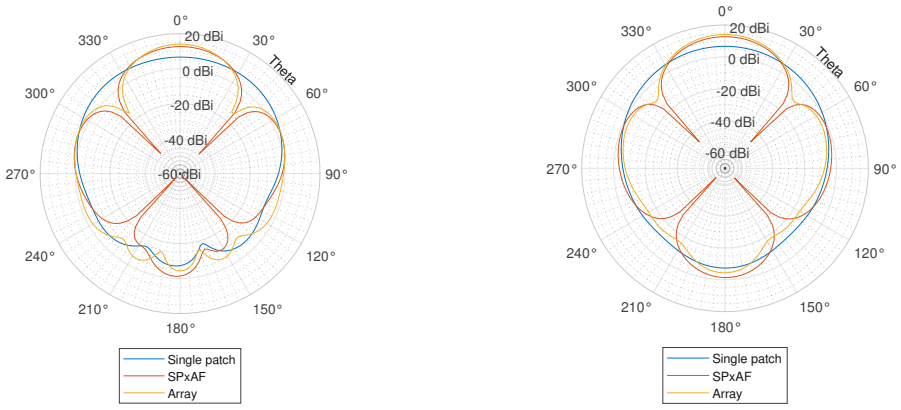

(a) $\Phi = 90°$ (b) $\Phi = 0°$

Fig. 3.8: Total realized gain of the proximity-fed antenna on Duroid substrate

	Singele patch	Array factor	Simulated array
$G_{\text{re,max}}$	6.61 dBi	12.6 dBi	14 dBi
$G_{\text{re,grating}}$	N/A	-1.1 dB	-3.2 dB
$G_{\text{re,back}}$	-7.38 dB	-1.43 dB	-4.39 dB

Tab. 3.8: Peak, grating lobe peak, back lobe total realized gain for proximity-fed array on Duroid substrate for $\Phi = 0°$

	Singele patch	Array factor	Simulated array
$G_{\text{re,max}}$	6.72 dBi	12.6 dBi	14 dBi
$G_{\text{re,grating}}$	N/A	2.38 dB	2.72 dB
$G_{\text{re,back}}$	-7.38 dB	-1.43 dB	-4.39 dB

Tab. 3.9: Peak, grating lobe peak, back lobe total realized gain for proximity-fed array on Duroid substrate for $\Phi = 90°$

Figure 3.8, tables 3.8 and 3.9 show that the increase of the total realized gain, from the single patch antenna to the array is from 6.61 dBi to 14 dBi that is larger than the predicted value of the pattern multiplication with the array factor which is 12.6 dBi.

The side lobe level is $SLL = 17.2$ dB for $\Phi = 0°$ and $SLL = 11.08$ dB for $\Phi = 90°$ which are better than the predicted $SLL = 13.7$ dB for $\Phi = 0°$ and $SLL = 10.22$ dB for $\Phi = 90°$.

	Single Patch	Array factor	Array
$\Phi = 0°$	84°	40°	36°
$\Phi = 90°$	122°	44°	36°

Tab. 3.10: Half-power beam-width of the proximity-fed antenna on Duroid substrate

From table 3.10, it can be seen that the resulting beam of the proximity-fed array is symmetric across the $\phi = 0°$ and $\phi = 90°$ planes.

3.4 Aperture-fed antennas on Duroid substrate

In this section, the aperture-fed patch antenna is compared to the simulated array, and the expected results acquired by the pattern multiplication with the array factor. These antennas are realized on the Duroid PCB substrate.

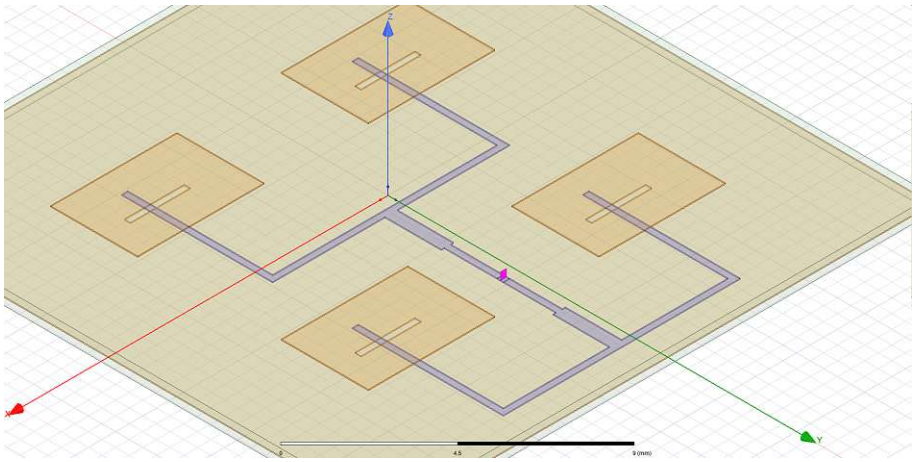

Fig. 3.9: HFSS model of the aperture-fed patch antenna array

In figure 3.9 the HFSS model of the aperture-fed patch antenna array is illustrated. In the model the purple rectangle in the middle of the feeding structure is the input port.

Dimension	Single Patch	Array	Unit
W_p	4.647	4.647	mm
L_p	3.395	3.201	mm
L_{stub}	1.983	1.2	mm
L_s	1.864	2.2	mm
W_s	0.186	0.22	mm
H_1	0.254	0.254	mm
H_2	0.254	0.254	mm

Tab. 3.11: Dimensions of aperture-fed patch antennas on Duroid substrate

When transitioning from the single patch configuration to the 2x2 planar array configuration the reoptimization of the aperture fed patch antenna took most effort because the coupling of the antenna is given by aperture length, but varying aperture length also affects frequency and therefore introduces a more complex reoptimization process.

S11 and VSWR

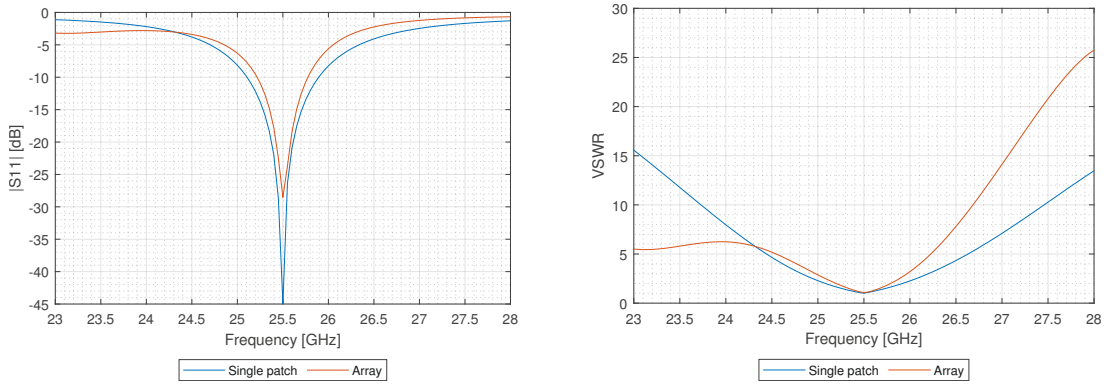

(a) $|\ S_{11}\ |$ (b) VSWR

Fig. 3.10: $|\ S_{11}\ |$ and VSWR of the aperture-fed antenna on Duroid substrate

Dimension	Single Patch	Array	Unit
$\|\ S_{11}\ \|_{\text{Upper}}$	25.893	25.8	GHz
$\|\ S_{11}\ \|_{\text{Lower}}$	25.105	25.3	GHz
$VSWR_{\text{Upper}}$	25.92	25.816	GHz
$VSWR_{\text{Lower}}$	25.08	25.275	GHz
BW	788	500	MHz

Tab. 3.12: Frequency limits of the aperture-fed antennas on Duroid substrate

From table 3.12 the frequency limits of the single patch antenna and of the resulting 2x2 array can be seen. The bandwidth for the single element patch antenna is 788 MHz and for the resulting array it is 500 MHz, that is decrease of 288 MHz, that corresponds to 36.5% decrease.

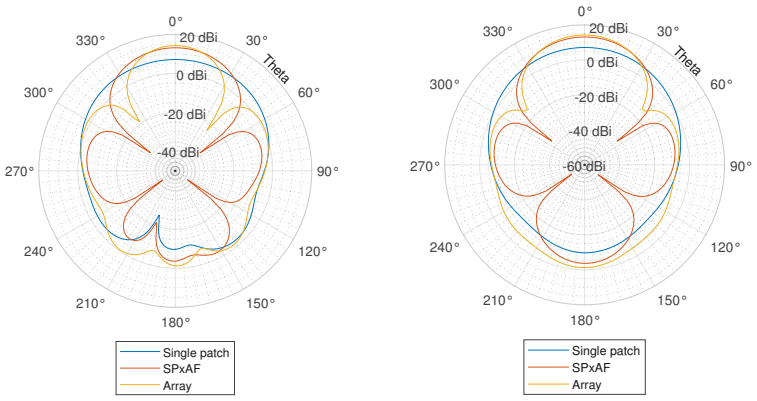

(a) $\Phi = 90°$ (b) $\Phi = 0°$

Fig. 3.11: Total realized gain of aperture-fed antenna on Duroid substrate

	Singele patch	Array factor	Simulated array
$G_{\text{re,max}}$	7.09 dBi	13.1 dBi	14.2 dBi
$G_{\text{re,grating}}$	N/A	-7.36 dB	-3.99 dB
$G_{\text{re,back}}$	-9.77 dB	-3.71 dB	-1.32 dB

Tab. 3.13: Peak, grating lobe peak, back lobe total realized gain for proximity-fed array on Duroid substrate for $\Phi = 0°$

	Singele patch	Array factor	Simulated array
$G_{\text{re,max}}$	7.09 dBi	13.1 dBi	14.2 dBi
$G_{\text{re,grating}}$	N/A	-3.99 dB	1.43 dB
$G_{\text{re,back}}$	-9.77 dB	-3.71 dB	-1.32 dB

Tab. 3.14: Peak, grating lobe peak, back lobe total realized gain for proximity-fed array on Duroid substrate for $\Phi = 90°$

Figure 3.11, tables 3.13 and 3.14 show that the increase of the total realized gain from the single patch antenna to the array is from 7.09 dBi to 14.2 dBi that is close to the expected value which is 13.1 dBi.

The side lobe level is $SLL = 18.19\ dB$ for the $\phi = 0°$ and $SLL = 12.77\ dB$ for the $\phi = 90°$ which is worse than the predicted $SLL = 20.46\ dB$ for $\phi = 0°$ and also worse than the predicted $SLL = 16.81\ dB$ for $\phi = 90°$.

	Single Patch	Array factor	Array
$\Phi = 0°$	80°	44°	40°
$\Phi = 90°$	110°	48°	32°

Tab. 3.15: Half-power beam-width of the aperture-fed antenna on Duroid substrate

From table 3.15 it can be seen that the resulting beam is tighter than the beam predicted by the multiplication of the single patch pattern with the array factor.

3.5 Inset-fed antennas on RT4530B substrate

In this section, the inset-fed patch antenna is compared to the simulated array, and the expected results acquired by the pattern multiplication with the array factor. These antennas are realized on the RO4350B PCB substrate.

Dimension	Single Patch	Array	Unit
W_p	3.854	3.854	mm
L_p	2.979	2.885	mm
y_0	0.964	1.301	mm
x_0	0.278	0.069	mm

Tab. 3.16: Dimensions of inset-fed patch antennas on RO4350B substrate

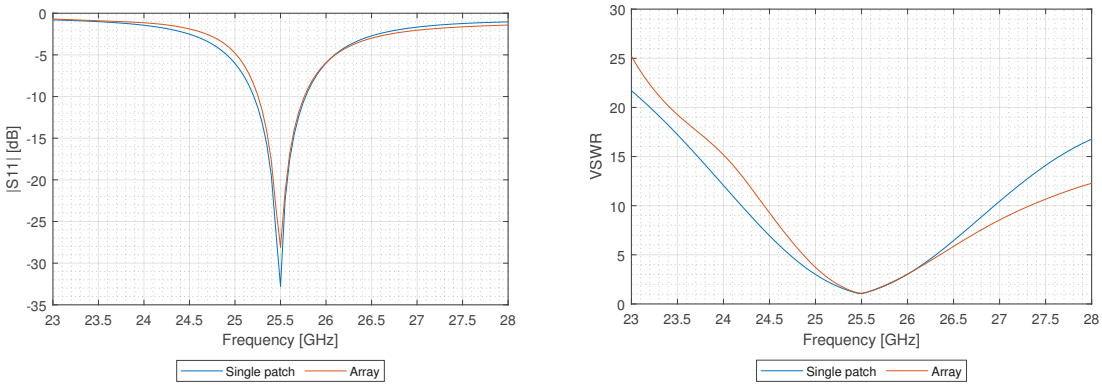

(a) $\mid S_{11} \mid$ (b) VSWR

Fig. 3.12: $\mid S_{11} \mid$ and VSWR of the inset-fed antenna on RO4350 substrate

Dimension	Single Patch	Array	Unit
$\mid S_{11} \mid_u$	25.776	25.762	GHz
$\mid S_{11} \mid_l$	25.206	25.254	GHz
$VSWR_U$	25.793	25.78	GHz
$VSWR_L$	25.189	25.24	GHz
BW	570	508	MGHz

Tab. 3.17: Frequency limits of the instet-fed antenna on RO4350 substrate

Table 3.17, shows the frequency limits of the single patch antenna and the resulting 2x2 antenna array. The bandwidth for the single patch is $BW = 570\ MHz$ and for the resulting array it is $BW = 508\ MHz$, which is 62 MHz smaller.

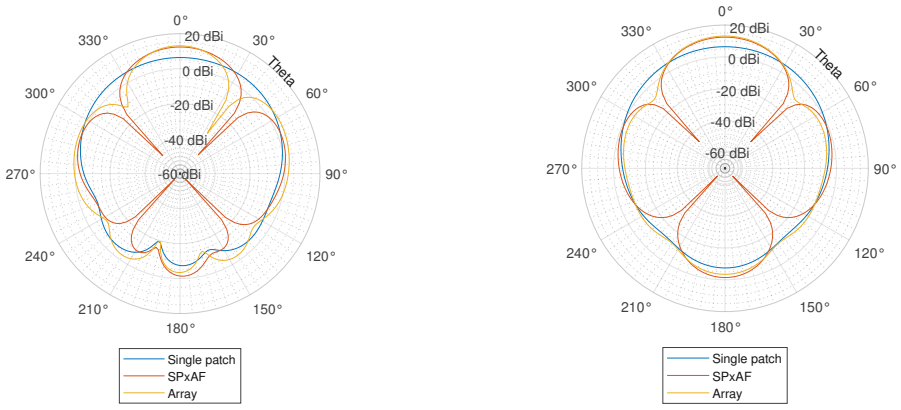

(a) $\Phi = 90°$ (b) $\Phi = 0°$

Fig. 3.13: Total realized gain of inset-fed antenna on RO4350 substrate

	Singele patch	Array factor	Simulated array
$G_{\text{re,max}}$	6.35 dBi	12.4 dBi	13.1 dBi
$G_{\text{re,grating}}$	N/A	-1.02 dB	-3.9 dB
$G_{\text{re,back}}$	-7.45 dB	-1.43 dB	-3.45 dB

Tab. 3.18: Peak, grating lobe peak, back lobe total realized gain for proximity-fed array on Duroid substrate for $\Phi = 0°$

	Singele patch	Array factor	Simulated array
$G_{\text{re,max}}$	6.35 dBi	12.4 dBi	13.1 dBi
$G_{\text{re,grating}}$	N/A	1.92 dB	4.37 dB
$G_{\text{re,back}}$	-7.79 dB	-1.43 dB	-3.45 dB

Tab. 3.19: Peak, grating lobe peak, back lobe total realized gain for proximity-fed array on Duroid substrate for $\Phi = 90°$

The figure 3.13, tables 3.18 and 3.19 show the values of the realized gain. From these values the side lobe level can be calculated. The side lobe level of the simulated array is 17 dB for $\phi = 0°$ and 8.73 dB for $\phi = 90°$, which is better than the expected value of 13.42 dB for $\phi = 0°$, but for $\phi = 90°$, the simulated is slightly bellow the expected value of 10.48 dB

	Single Patch	Array factor	Array
$\Phi = 0°$	88°	40°	38°
$\Phi = 90°$	112°	40°	32°

Tab. 3.20: Half-power beam-width of the inset-fed antenna on RO4350

From the table 3.20 it can be seen that the half power beam-width of the resulting 2x2 inset-fed patch antenna array is tighter than the expected, but is also less symmetric across the $\phi = 0°$ and $\phi = 90°$ planes.

3.6 Proximity-fed antennas on RT4530B substrate

In this section, the proximity-fed patch antenna is compared to the simulated array, and the expected results acquired by the pattern multiplication with the array factor. These antennas are realized on the RO4350B PCB substrate.

Dimension	Single Patch	Array	Unit
W_p	3.897	3.854	mm
L_p	2.833	2.803	mm
l_{stub}	2.074	2.076	mm

Tab. 3.21: Dimensions of the proximity-fed patch antennas on RO4350B substrate

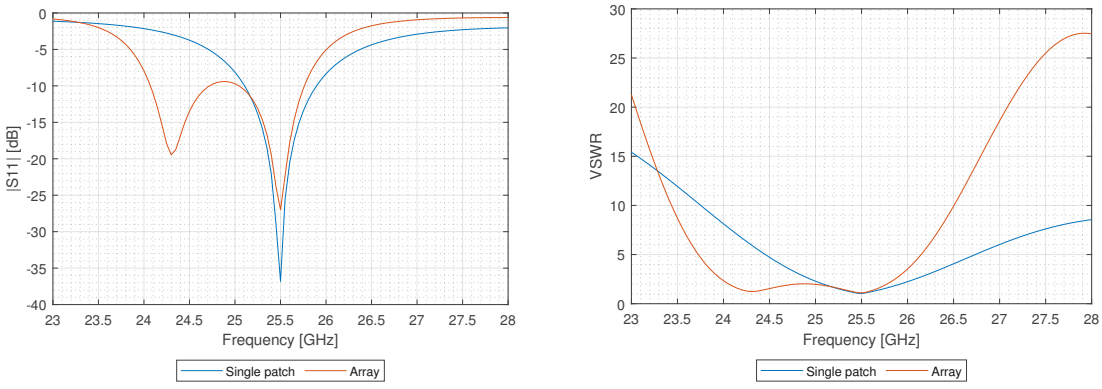

(a) | S_{11} | (b) VSWR

Fig. 3.14: | S_{11} | and VSWR of proximity-fed antenna on RO4350 substrate

Figure 3.14, shows the | S_{11} | and VSWR for the proximity-fed patch antenna. In the graph of | S_{11} |, there can be seen second resonance around 24.3 GHz, this resonance is caused by the microstrip stub, which radiates at this frequency.

Dimension	Single Patch	Array	Unit
$\mid S_{11} \mid_{\text{Upper}}$	25.896	25.761	GHz
$\mid S_{11} \mid_{\text{Lower}}$	25.105	25.05	GHz
$VSWR_{\text{Upper}}$	25.923	25.776	GHz
$VSWR_{\text{Lower}}$	25.083	24.96	GHz
BW	791	711	MHz

Tab. 3.22: Frequency limits of the proximity-fed antennas on RO4350 substrate

From table 3.22 the bandwidth of the single patch and the resulting array, can be calculated. The bandwidth for the single patch is $BW = 791\ MHz$ and for the resulting 2x2 array the bandwidth is $BW = 711\ MHz$, that is a 80 MHz decrease of the bandwidth.

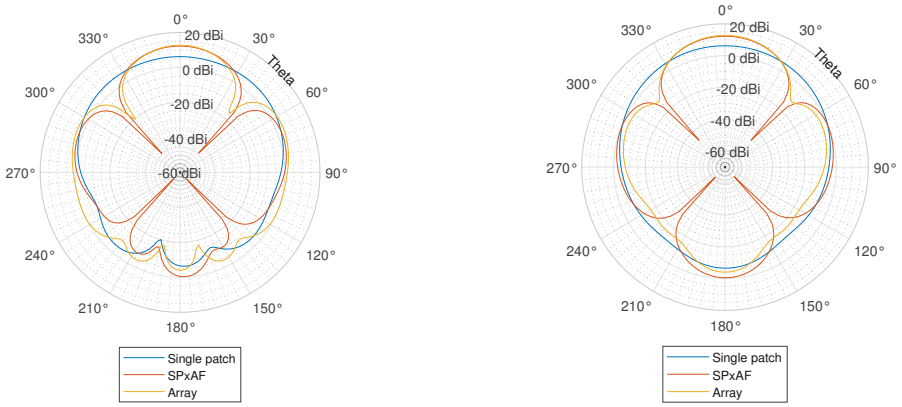

(a) $\Phi = 90°$ (b) $\Phi = 0°$

Fig. 3.15: Total realized gain of the proximity-fed antenna on RO4350 substrate

	Singele patch	Array factor	Simulated array
$G_{\text{re,max}}$	6.18 dBi	12.2 dBi	12.7 dBi
$G_{\text{re,grating}}$	N/A	$-0.37\ dB$	$-3.75\ dB$
$G_{\text{re,back}}$	$-6.55\ dB$	$-0.534\ dB$	$-4.04\ dB$

Tab. 3.23: Peak, grating lobe peak, back lobe total realized gain for proximity-fed array on Duroid substrate for $\Phi = 0°$

	Singele patch	Array factor	Simulated array
$G_{\text{re,max}}$	6.18 dBi	12.2 dBi	12.7 dBi
$G_{\text{re,grating}}$	N/A	2.38 dB	4.14 dB
$G_{\text{re,back}}$	-6.33 dB	-0.534 dB	-4.04 dB

Tab. 3.24: Peak, grating lobe peak, back lobe total realized gain for proximity-fed array on Duroid substrate for $\Phi = 90°$

Figure 3.15, tables 3.23 and 3.24 show that the increase of the total realized gain, from the single patch antenna to the array is from 6.18 dBi to 12.7 dBi that is close to the predicted value which is 12.2 dBi.

The side lobe level is $SLL = 16.45$ dB for $\phi = 0°$ and $SLL = 8.56$ dB for $\phi = 90°$ which is better than the predicted values of $SLL = 12.57$ dB for $\phi = 0°$ and slightly bellow $SLL = 9.82$ dB for $\phi = 90°$.

	Single Patch	Array factor	Array
$\Phi = 0°$	96°	40°	40°
$\Phi = 90°$	124°	40°	36°

Tab. 3.25: Half-power beam-width of the proximity-fed antenna on RO4350

The beam-width of the array is close to the predicted but for $\phi = 90°$ it is 4° tighter.

3.7 Aperture-fed antennas on RT4530B substrate

In this section, the aperture-fed patch antenna is compared to the simulated array, and the expected results acquired by the pattern multiplication with the array factor. These antennas are realized on the RO4350B PCB substrate.

Dimension	Single Patch	Array	Unit
W_p	3.850	3.854	mm
L_p	2.6350	2.194	mm
L_{stub}	1.7557	0.902	mm
L_s	1.6776	1.993	mm
W_s	0.1677	0.199	mm

Tab. 3.26: Dimensions of the aperture-fed patch antennas on RO4350B substrate

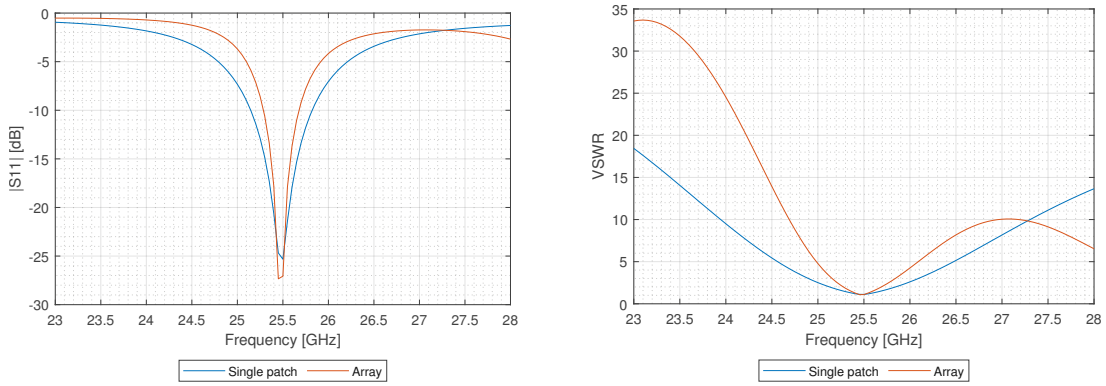

(a) $|\ S_{11}\ |$ (b) VSWR

Fig. 3.16: $|\ S_{11}\ |$ and VSWR of aperture-fed antenna on RO4350 substrate

Dimension	Single Patch	Array	Unit
$\|\ S_{11}\ \|_{\text{Upper}}$	25.822	25.686	GHz
$\|\ S_{11}\ \|_{\text{Lower}}$	25.147	25.270	GHz
$VSWR_{\text{Upper}}$	25.850	25.696	GHz
$VSWR_{\text{Lower}}$	25.148	25.259	GHz
BW	675	416	MHz

Tab. 3.27: Frequency limits of the aperture-fed antennas on RO4350 substrate

From table 3.22 the frequency limits of the single patch antenna and the resulting 2x2 array can be seen. The bandwidth for the single patch is $BW = 675\ MHz$ and for the resulting 2x2 array the bandwidth is $BW = 416\ MHz$, that is 259 MHz decrease of the bandwidth, which is significant.

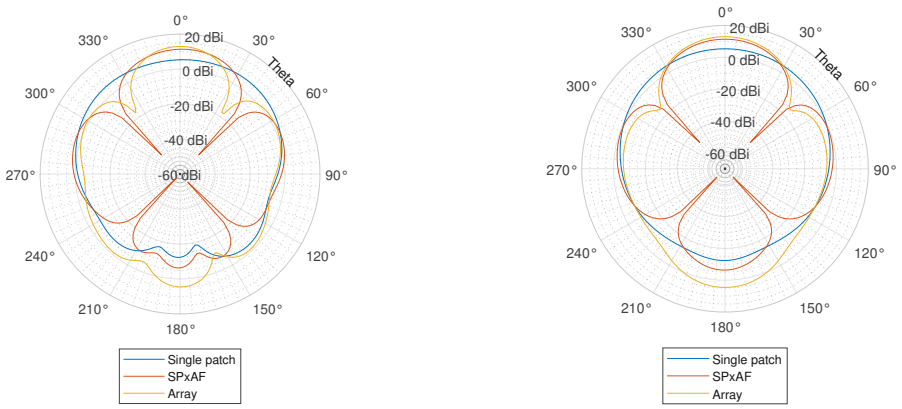

(a) $\Phi = 90°$ (b) $\Phi = 0°$

Fig. 3.17: Total realized gain of the aperture-fed antenna on RO4350 substrate

	Singele patch	Array factor	Simulated array
$G_{\text{re,max}}$	5.31 dBi	11.3 dBi	12.9 dBi
$G_{\text{re,grating}}$	N/A	-0.7 dB	-5.16 dB
$G_{\text{re,back}}$	-12.4 dB	-6.37 dB	4.52 dB

Tab. 3.28: Peak, grating lobe peak, back lobe total realized gain for proximity-fed array on Duroid substrate for $\Phi = 0°$

	Singele patch	Array factor	Simulated array
$G_{\text{re,max}}$	6.03 dBi	11.4 dBi	12.9 dBi
$G_{\text{re,grating}}$	N/A	2.86 dB	1.44 dB
$G_{\text{re,back}}$	-12.39 dB	-6.33 dB	4.52 dB

Tab. 3.29: Peak, grating lobe peak, back lobe total realized gain for proximity-fed array on Duroid substrate for $\Phi = 90°$

Figure 3.17, tables 3.28 and 3.29 show that the gain increase from the single patch antenna to the array is from 5.31 dB to 12.9 dB that is larger than the predicted value which is 11.4 dB.

The side lobe level is $SLL = 18.06$ dB for $\phi = 0°$ and $SLL = 11.46$ dB for $\phi = 90°$ which is significantly better than the predicted $SLL = 12$ dB for $\phi = 0°$ and slightly better than the predicted $SLL = 8.54$ dB for $\phi = 90°$.

	Single Patch	Array factor	Array
$\Phi = 0°$	98°	40°	40°
$\Phi = 90°$	130°	44o	36°

Tab. 3.30: Half-power beam-width of the aperture-fed antenna on RO4350 substrate

For $\phi = 0°$ the half power beam-width has the same width as the predicted, but for $\phi = 90°$ the beam-width is tighter by 9°.

4 Comparison of 2x2 patch antenna arrays

This chapter is dedicated to the comparison of patch antenna arrays.

4.1 Comparison of 2x2 antenna array on Duroid substrate

This section focuses on comparison of different feeding techniques for 2x2 patch antenna arrays realized on Duroid substrate.

4.1.1 S11 and VSWR

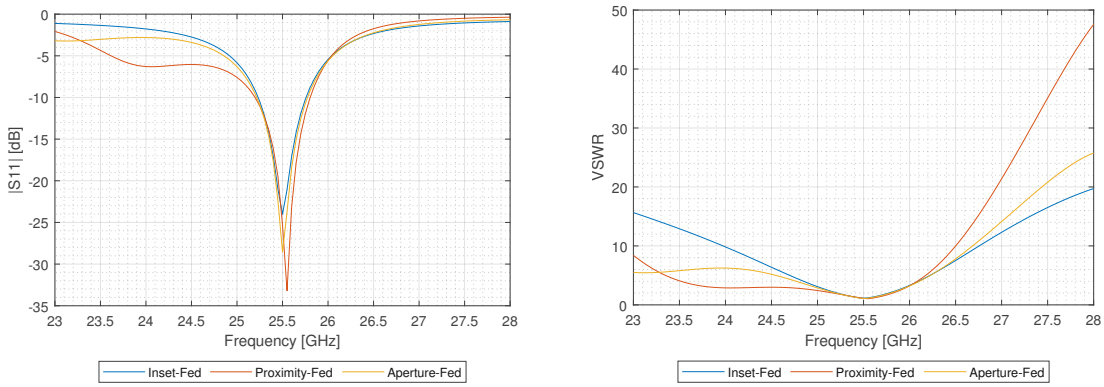

(a) | S_{11} | (b) VSWR

Fig. 4.1: | S_{11} | and VSWR of 2x2 antenna arrays on Duroid substrate

	Inset-fed	Proximity-fed	Aperture-fed
$BW_{\mathrm{S1,1}}$	527 MHz	600 MHz	500 MHz
BW_{VSWR}	559 MHz	651 MHz	541 MHz

Tab. 4.1: Bandwidth of 2x2 arrays on Duroid substrate

From table 4.1 it can be seen that the largest bandwidth in respect of $S_{1,1}$ and VSWR has the proximity fed array. The second largest is by the inset-fed patch antenna array and the smallest by the aperture-fed patch antenna array. This order is different from the single patch case where the aperture-fed patch antenna shows the best result.

4.1.2 Antenna gain

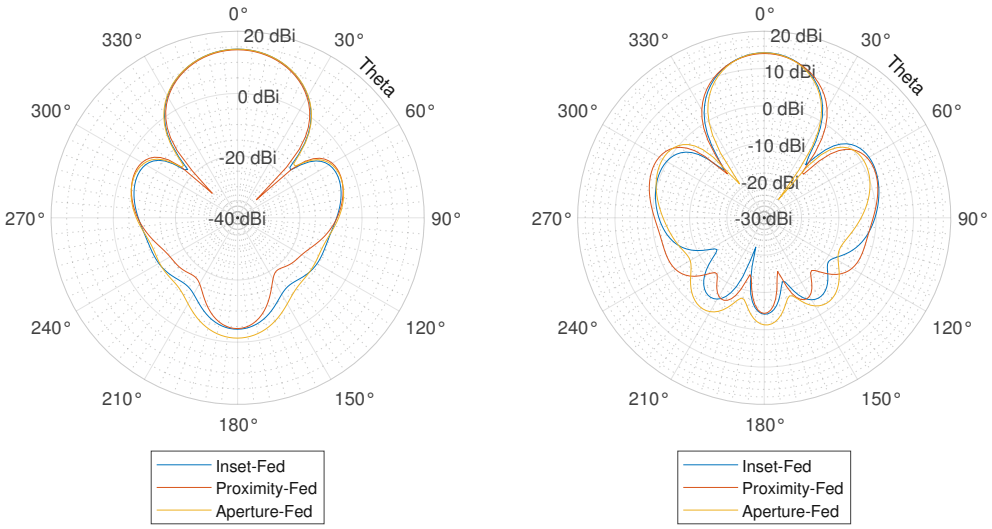

(a) $\Phi = 0°$ (b) $\Phi = 90°$

Fig. 4.2: Co-polarized component of the realized gain of Duroid patch antenna arrays

From the gain pattern, it can be seen that the aperture-fed patch antenna array has the largest level of back radiation. The front to back ratio of the aperture-fed patch antenna is 15.5 dB. The inset-fed and proximity fed have the front to back ratio at the same level of 18.4 dB, which is significantly better than the case for aperture-fed patch antenna.

The realized gain in the direction of broadside $\theta = 0°$ is 14.2 dBi for inset-fed array, 14 dBi for proximity-fed array and 14.2 dBi for aperture coupled array.

The side lobe levels of the antenna arrays are the following: for $\phi = 0°$ plane the inset-fed array has $SLL = 18.2\ dB$, for the proximity-fed array the $SLL = 17.2\ dB$ and for the aperture-fed array the $SLL = 18.2\ dB$. For $\phi = 90°$ plane the insed-fed patch array has $SLL = 11.71\ dB$, the proximity fed patch array has the $SLL = 11.08\ dB$ and the aperture-fed array has $SLL = 12.77\ dB$. In case the side lobe level is concerned the best performance offers the aperture-fed array.

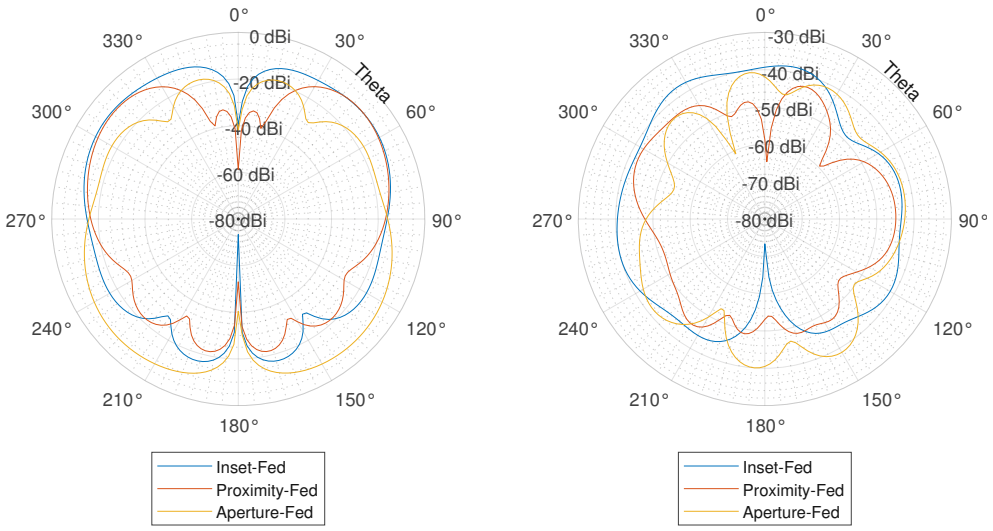

(a) $\Phi = 0°$ (b) $\Phi = 90°$

Fig. 4.3: Cross-polarized component of the realized gain of Duroid patch antenna arrays

From the cross polarized component of the gain, it can be seen that for the $\phi = 0°$ the proximity fed patch antenna has the smallest gain of the cross-polarized component along the angle of its beamwidth. This is also valid for the $\phi = 90°$ plane. The second best performs the aperture-fed antenna array.

	Inset-fed	Proximity-fed	Aperture-fed
$\Phi = 0°$	32°	36°	32°
$\Phi = 90°$	36°	36°	40°

Tab. 4.2: Half-power beam-width of arrays on Duroid substrate

The tightest beam is produced by the inset-fed patch antenna array, but the proximity-fed array exhibits the most symmetric beam over the $\Phi = 0°$ and the $\Phi = 90°$ plane.

Frequency	25 GHz	25.25 GHz	25.5 GHz	25.75 GHz	26 GHz
Inset-fed	12.828 dBi	13.899 dBi	14.313 dBi	13.788 dBi	12.542 dBi
Proximity-fed	13.34 dBi	13.81 dBi	14.01 dBi	13.48 dBi	12.01 dBi
Aperture-fed	12.546 dBi	13.657 dBi	14.215 dBi	13.871 dBi	12.777 dBi

Tab. 4.3: Duroid antenna arrays peak total realized gain over frequency

.

Over the frequency band, the gain is best for the inset-fed patch antenna array.

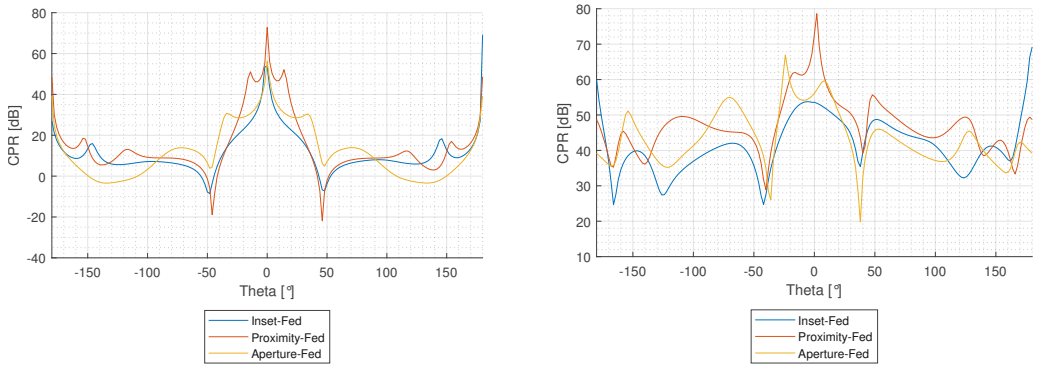

(a) $\Phi = 0°$ (b) $\Phi = 90°$

Fig. 4.4: Cross Polarization Ratio of arrays on Duroid substrate

Over the half power beam-width for the $\phi = 0°$ plane the inset-fed array has a cross polarization ratio above 24 dB , the proximity-fed array has a cross polarization ratio above 40.8 dB and the aperture-fed array has a cross polarization ratio over 29.9 dB. For the $\phi = 90°$ plane the inset-fed array has a cross polarization ratio over 49.5 dB, the proximity-fed array over 53.6 dB and the aperture-fed array has a cross polarization ratio over 50.7 dB.

From the cross polarization ratio aspect, the best performance over its beam-width shows the proximity fed patch antenna, the aperture-fed patch antenna array comes second, and the inset-fed patch antenna last.

4.1.3 Antenna efficiency

Frequency	25 GHz	25.25 GHz	25.5 GHz	25.75 GHz	26 GHz
Inset-fed	0.941	0.947	0.946	0.938	0.924
Proximity-fed	0.939	0.934	0.917	0.890	0.856
Aperture-fed	0.914	0.921	0.924	0.923	0.920

Tab. 4.4: Duroid antenna arrays efficiency over frequency

The highest overall efficiency over the frequency band has the inset-fed patch antenna array.

4.2 Comparison of 2x2 antenna array on RO4350 substrate

This section focuses on the comparison of different feeding techniques for 2x2 patch antenna arrays realized on RO4350 substrate.

4.2.1 S11 and VSWR

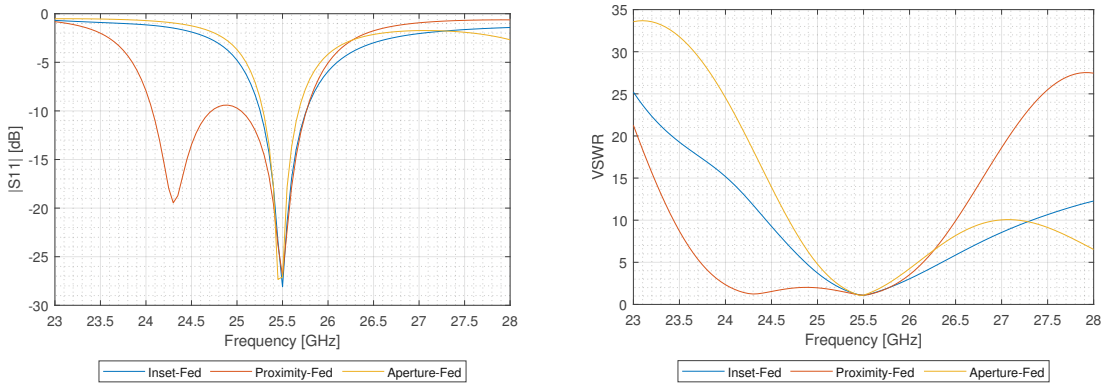

(a) $\mid S_{11} \mid$ (b) VSWR

Fig. 4.5: $\mid S_{11} \mid$ and VSWR of the 2x2 antenna arrays on RO4350 substrate

Figure 4.5 shows that the proximity-fed patch antenna exhibits second resonance caused by the matching stub. Other feeding methods don't exhibit this second resonance.

	Inset-fed	Proximity-fed	Aperture-fed
$BW_{\mathrm{S1,1}}$	508 MHz	711 MHz	416 MHz
BW_{VSWR}	540 MHz	816 MHz	437 MHz

Tab. 4.5: The bandwidth of the 2x2 arrays on RO4350 substrate

The largest bandwidth exhibits the proximity-fed patch antenna, which is concurrent with the case for the single patch configuration. Unlike the single patch configuration, the second largest bandwidth exhibits the inset-fed patch antenna. Which is unlike in the case of a single patch, where the second largest bandwidth was exhibited by the aperture-fed patch antenna.

4.2.2 Antenna gain

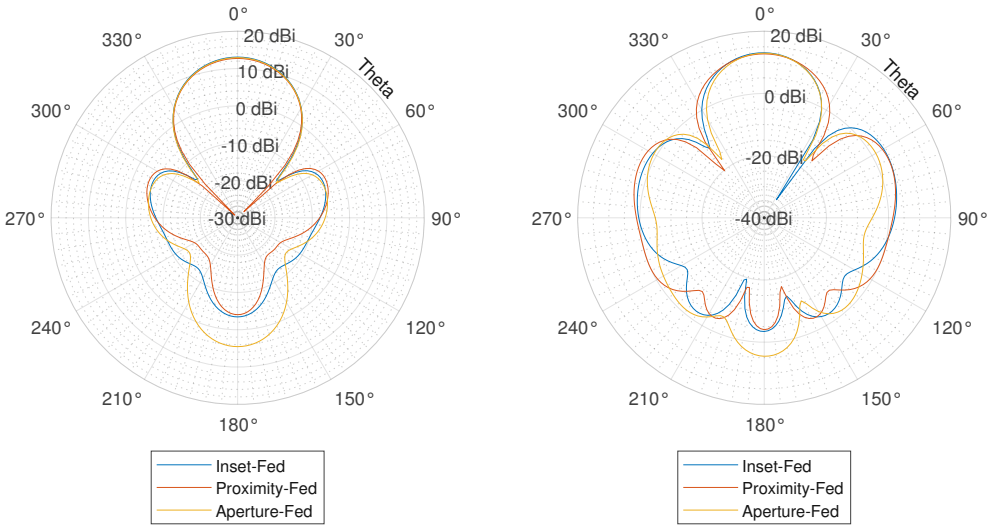

(a) $\Phi = 0°$ (b) $\Phi = 90°$

Fig. 4.6: Co-polarized component of the realized Gain of RO450B patch antenna arrays

From the antenna gain pattern, it can be seen that the aperture-fed patch antenna array has the largest back radiation and the proximity patch antenna array has the smallest. It can also be seen that the gratings lobes generated by the aperture-fed patch antenna are comparatively smaller than the grating lobes generated by the other arrays.

The front to back ratio of the inset-fed patch antenna array is 18.37 dB, for the proximity-fed array, it is 16.74 dB and for the aperture-fed array, it is 17.42 dB. From these values, it can be seen that the proximity-fed array exhibits the least backward radiation.

The side lobe level of the inset fed patch antenna is 17 dB for $\phi = 0°$ and 8.73 dB for $\phi = 90°$. For the proximity-fed antenna array it is 16.45 dB for $\phi = 0°$ and 8.56 dB for $\phi = 90°$ and for the aperture-fed antenna array it is 18.06 dB for $\phi = 0°$ and 11.46 dB for $\phi = 90°$. In the case the side lobe level is concerned the best performance offers the aperture-fed array.

	Inset-fed	Proximity-fed	Aperture-fed
$\Phi = 0°$	38°	40°	36°
$\Phi = 90°$	32°	36°	32°

Tab. 4.6: Half-power beam-width of arrays on RO4350B substrate

From the table 4.6, it can be seen that the tightest beam belongs to the inset-fed array, whereas the aperture-fed array has the tightest.

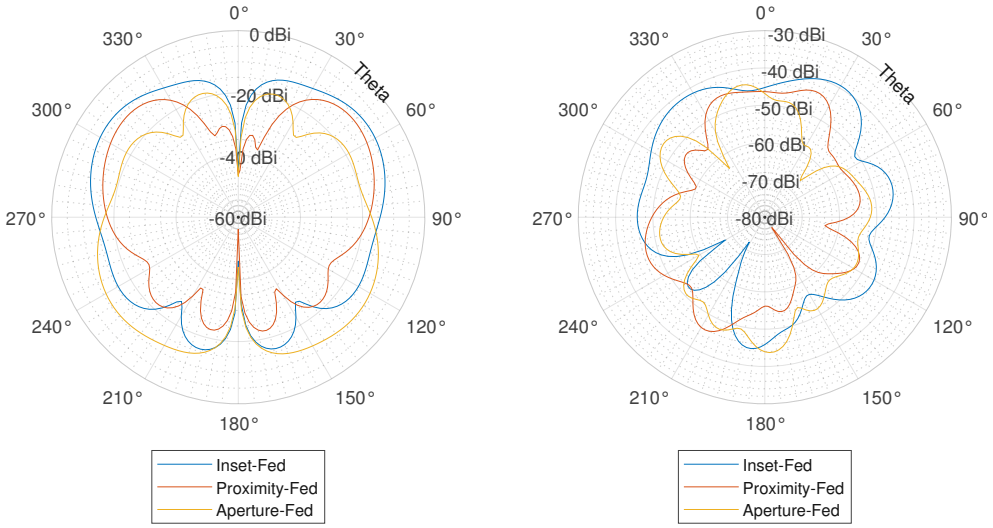

(a) $\Phi = 0°$ (b) $\Phi = 90°$

Fig. 4.7: Cross-polarized component of the realized Gain of RO450B patch antenna arrays

Frequency	25 GHz	25.25 GHz	25.5 GHz	25.75 GHz	26 GHz
Inset-fed	11.04 dB	12.60 dB	13.13 dB	12.59 dB	11.56 dB
Proximity-fed	12.53 dB	12.72 dB	12.71 dB	11.99 dB	10.42 dB
Aperture-fed	10.21 dB	11.73 dB	12.38 dB	11.62 dB	9.99 dB

Tab. 4.7: RO4350B antenna arrays peak total realized gain over frequency

.

The best gain over frequency exhibits the inset-fed array, but over the lower frequencies, the proximity-fed array performs better.

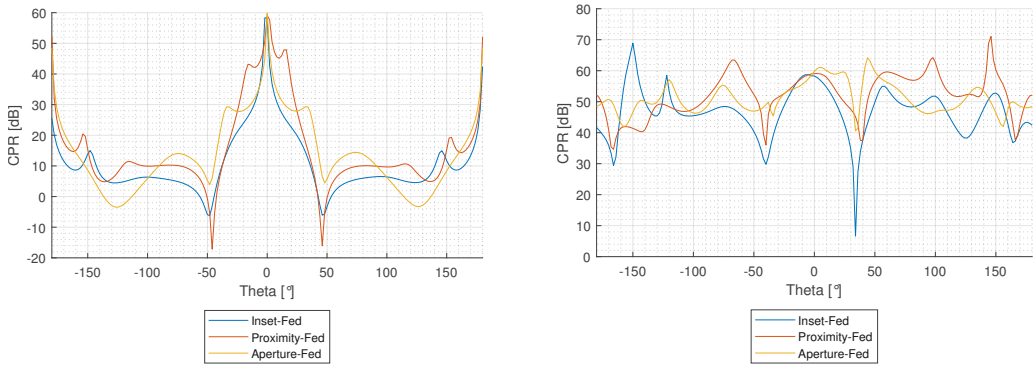

(a) $\Phi = 0°$ (b) $\Phi = 90°$

Fig. 4.8: Cross Polarization Ratio of RO450B patch antenna arrays

Over the angle of the beam for $\Phi = 0°$ the inset-fed array has a cross polarization ration higher than 22 dB, the proximity-fed array has a cross polarization ration over 40.9 dB and the aperture-fed array over 29.2 dB. For $\Phi = 90$ over the respective beam-width the inset-fed array has a cross polarization over 50.8 dB, the proximity-fed array has a cross polarization ratio over 54.68 dB and the aperture-fed array has over 58.27 dB.

This means that for the $\Phi = 0°$ plane, the proximity-fed array has the best performance over its half-power beam-width, and for the $\Phi = 90°$ plane, the best performance over its beam-width exhibits the aperture-fed array.

4.2.3 Antenna efficiency

Frequency	25 GHz	25.25 GHz	25.5 GHz	25.75 GHz	26 GHz
Inset-fed	0.722	0.766	0.787	0.782	0.756
Proximity-fed	0.831	0.811	0.774	0.726	0.674
Aperture-fed	0.744	0.745	0.739	0.725	0.707

Tab. 4.8: Efficiency over frequency of 2x2 antenna arrays on RO4350B substrate

The most uniform efficiency over the frequency band exhibits the inset-fed array, followed by the proximity-fed array.

Conclusion

The comparison of single patch antenna elements was realized on Rogerscorp RT/-Duroid 5880 and the Rogerscorp RO4350B. Out of the single patch antennas, the aperture-fed patch antennas exhibit the largest bandwidth, which in the array configuration is substantially lower. This decrease of bandwidth is largest in the case of the aperture-fed patch antenna.

The inset-fed patch antennas exhibit a good cross polarization ratio, but the aperture-fed and proximity-fed patch antennas perform better. This is also true in the case of the extension to the 2x2 array.

After comparing the 2x2 patch antenna arrays realized on two different substrates, it is apparent that the bandwidth of the proximity patch antenna arrays performs the best. They also show very good results in cross polarization ratio, where they perform the best across the angle of their half-power beam for the $\phi = 0°$ plane. In the $\phi = 90°$ plane, they also exhibit very good performance. Cross polarization wise the worst performance exhibits the inset-fed array. The proximity-fed patch antenna arrays also exhibit low backward radiation levels.

The main difference between the arrays realized on the Duroid substrate and the RO4350B substrate is that the bandwidth is lower on the RO4350B substrate, which is also true about the gain. This is caused by higher dielectric losses of the RO4350B substrate, whereas the Duroid substrate has small dielectric losses. The small dielectric losses of the Duroid substrate are responsible for the fact that the gains of the arrays on Duroid substrate are almost the same. There is also a difference in front to back ratio of the aperture-fed patch antenna, which is caused by the size of the aperture.

If larges bandwidth is required, the best choice is the proximity-fed patch antenna array. In the case the largest gain is required, the inset-fed patch antenna should be selected. If a large sidelobe level is required, the best choice is the aperture-fed patch antenna. If a large cross polarization ratio is required, the best choice would be the proximity-fed patch antenna.

Bibliography

[1] Constatine A. Balanis. *Antenna Theory: Analysis and Design, 4th Edition*. John Wiley, Febuary 2016.

[2] A. Ludwig. The definition of cross polarization. *IEEE Transactions on Antennas and Propagation*, 21(1):116–119, 1973. doi:10.1109/TAP.1973.1140406.

[3] Terry C. Edwars and Michael B. Steer. *Foundations for Microstrip Circuit Design*. Wiley-IEEE Press, USA, 2016.

[4] Saleh Eesaa, M.A. Jusoh, Muhammad Hafiz, and Sumodro Mahmud. Finding the best feeding point location of patch antenna using hfss. *ARPN Journal of Engineering and Applied Sciences*, 10:17444–17449, January 2015.

[5] Quarter-Wavelength Transmission Line, 3 2021. [Online; accessed 2021-07-09]. URL: https://eng.libretexts.org/@go/page/6285.

[6] Microstrip Transmission Lines, 3 2021. [Online; accessed 2021-07-02]. URL: https://eng.libretexts.org/@go/page/41029.

[7] D.M. Pozar and B. Kaufman. Increasing the bandwidth of a microstrip antenna by proximity coupling. *Electronics Letters*, 23(8):368 – 369, 1987. doi:10.1049/el:19870270.

[8] D.M Pozar. A review of aperture coupled microstrip antennas: History, operation, development, and applications. 1996.

[9] F. Caspers. Rf engineering basic concepts: S-parameters, 2012. arXiv:1201.2346.

[10] Constantine A. Balanis. *Fundamental Parameters and Definitions for Antennas*, chapter 1, pages 1–56. John Wiley & Sons, Ltd, 2008. doi:https://doi.org/10.1002/9780470294154.

[11] Ieee standard for definitions of terms for antennas. *IEEE Std 145-2013 (Revision of IEEE Std 145-1993)*, pages 1–50, 2014. doi:10.1109/IEEESTD.2014.6758443.

[12] Nafati A. Aboserwal, J. Salazar, J. A. Ortíz, José. Díaz, C. Fulton, and R. Palmer. Source current polarization impact on the cross-polarization definition of practical antenna elements: Theory and applications. *IEEE Transactions on Antennas and Propagation*, 66:4391–4406, 2018.

Symbols and abbreviations

QWIT	Quarter Wave Impedance Transformer
f_r	resonant frequency
C_0	speed of the light
ϵ_{eff}	effective permittivity
ϵ_r	relative permittivity
ϵ_0	permittivity of vacuum
W_p	width of the patch
L_p	length of the patch
L_{eff}	effective length of the patch
VSWR	voltage standing wave ration
SLL	Side lobe level
h	substrate thickness
ΔL	length extension
L_{stub}	length of the stub
Γ	reflection coefficient
A_e	effective equivalent area
A_c	capture equivalent area
A_L	loss equivalent area
A_S	scattering equivalent area
L_S	length of the slot
W_S	width of the slot
PTFE	Polytetrafluorethylen
PCB	printed circuit board
h	height of the substrate

w	width of the microstrip line
HEM	hybrid electromagnetic
TEM	transverse electromagnetic
R_{in}	edge resistance
ϵ_{AP}	aperture efficiency
A_P	physical area of the antenna
W_i	power density of incident wave
R_L	loss resistance
R_R	radiation resistance
$D(\theta, \phi)$	directivity
D_{max}	maximum directivity
$G(\theta, \phi)$	gain
G_{max}	peak gain
$G_{\text{re}}(\theta, \phi)$	realized gain
$G_{\text{re,max}}$	peak realized gain
η_0	overall efficiency
η_r	reflection efficiency
η_c	conduction efficiency
η_d	dielectric efficiency
P_{Rad}	radiated power
$AF(\theta, \phi)$	array factor
Z_0	characteristic impedance
$U(\theta, \phi)$	radiation intensity